Drop Impact on Fabrics

Ali Mozafari

A THESIS SUBMITTED TO
THE FACULTY OF GRADUATE STUDIES
IN PARTIAL FULFILLMENT OF THE REQUIREMENTS
FOR THE DEGREE OF
MASTER OF APPLIED SCIENCE

Graduate Program in Mechanical Engineering
York University
Toronto, Ontario

January 2020

Abstract

Drop impact has been studied mostly for systems that are rough, porous, or deformable. Limited research on drop impact onto fabrics is available. Here, drop impact on fabrics is studied to understand whether fabrics' features can change the dynamics of droplet. This study is done to develop a model to describe drop impact on fabrics. Five different woven fabrics are examined at different tensions. High speed images of the phenomena are analyzed to study spreading shape of droplet and measure its maximum diameter. Higher waviness (key factor) of fabric results in decrease in maximum spreading of droplet. Most part of the initial energy of droplet will be transformed to the surface energy of droplet at maximum spreading. Also, due to small fabric deflection and small void size, droplet behavior does not change drastically by changing fabric tension or void size and the energy loss of the droplet is not considerable.

Dedication

This thesis is dedicated to my parents, Reza and Mitra. I have to thank my parents for their love and support throughout my life and education.

Acknowledgments

I am grateful to my supervisor, Prof. Alidad Amirfazli, for his endless support and generous guidance. I consider myself a very lucky student as I had a chance to work under his supervision where I learned how to think properly and to make thought accessible.

Table of Content

List of Tables

List of Figures

Chapter I: Introduction

Drop impact on fabrics is of special importance due to exposure of clothing to rain, aerosolized chemical agents, or in a printing process. For example, in inkjet printing a droplet impacts and spreads on textiles. Also, the need for special protective clothing for occupations- like oil workers or military personnel necessitates the study of droplet impact on fabrics [1]. Despite these applications, complexity of drop dynamics on textile may have discouraged attention to this topic. Fabrics are porous, rough (weaved), flexible and have a variety of wettability. All such characteristics complicates drop impact dynamics on its own. Progress has been made in the literature in studies done for drop impact on porous surfaces or flexible surfaces that can help us in framing dynamics of droplet impact on fabrics. But, before that we should identify factors which are important in drop impact on non-porous and non-deformable surfaces. Based on studies which are done in the area of drop impact on non-porous and solid surfaces, wettability and roughness of surfaces are responsible for changing dynamics of droplet [2], amongst other factors such as drop impact velocity, liquid properties, and surrounding gas conditions.

Surface wettability is the ability of a liquid to maintain a contact with a solid surface. To characterize the surface wettability and to investigate its effect on the dynamics of drop impact, the approach which is mainly used by researchers is a dynamic approach, by means of drop impact studies. A wide range of works are dedicated to the investigation of drop impact on solid surfaces. There are many studies, either experimental, numerical, or

theoretical, that refer to surfaces with high wettability (i.e., hydrophilic or super-hydrophilic while droplet liquid is water), or low wettability (i.e., hydrophobic or super-hydrophobic while droplet liquid is water).

Among early studies of influence of wettability is the work by Hartley and Brunskill [3], who showed the role of wettability in drop rebound after impact onto leaves. They proposed an energy balance approach for the spreading droplet, in which the wettability was the main factor in droplet behavior. An approach to drop impact on super hydrophobic surfaces is given by Rioboo et al. [4], and four different outcomes were obtained: deposition, rebound, sticking, and fragmentation, and a drop impact regime map was suggested. They observed that, for the surfaces with low wettability (water drops on super hydrophobic polypropylene surface), the transition from rebound to fragmentation was governed by We value which is the ratio between the inertial forces and the surface tension force.

There are many inter-relationships between different parameters in drop impact that each of them affect droplet behavior. Antonini et al. [5] found that wettability of surfaces affects droplet maximum spreading and spreading characteristic time. Results from impact tests show that two different regimes can be seen for drop impact on surfaces. Weber number is the ratio between the inertial force and the surface tension force ($\rho.V^2/D$) that ρ is liquid density, V is the impact velocity and D is the diameter of droplet. For We numbers lower than 200, wettability affects both drop maximum spreading diameter ad time. But, for We numbers higher than 200, wettability effect is secondary, because capillary forces are overcome by inertial effects. In general, they showed that contact angle and contact angle hysteresis are fundamental parameters to study the effect of wettability on dynamics of droplet. They showed that at higher contact angles droplet spreading rate will be increased.

Based on these results, it can be assumed that wettability of fabrics would be important in spreading rate of droplet after impact. In other words, droplet will spread faster on fabrics which are hydrophobic.

Another important factor in determining droplet behavior on surfaces is surface roughness. The investigation of droplets impacting rough substrates is important and has received the attention of numerous researchers. So far, it is shown that rough surfaces trigger splashing and suppress corona splashing under various conditions. It has been observed that increasing the amplitude of the roughness increase probability of splashing and detachment of satellite droplet, which was also confirmed by Range and Feuillebois [6]. Wenzel [7] found that increasing roughness will enhance the wettability caused by the chemistry of surface, which means if the surface is hydrophobic, it will become even more hydrophobic when surface roughness is added. Besides, it was found that increasing roughness result in faster spreading of droplet and size and number of fingers at the rim will be increased and at the same time instabilities will be increased [4]. Figure 1.1, shows the splashing of droplet on a solid surface.

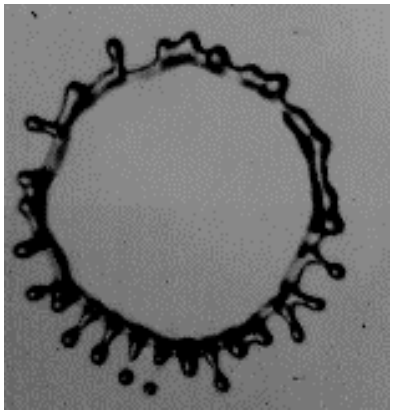

Figure 1.1: Droplet splashing on a solid surface

But, increasing roughness will not always increase probability of splashing. Waviness (discussed in Chapter 2) is one of the factors that affect droplet behavior. Waviness (undulation) refers to uneven surfaces that appear periodically at longer intervals than the roughness. Mundo et al. [8] studied droplet impact on rough disks and found that no corona splashing occurs after a droplet impacts a surface with waviness. Range and Feuillebois [6] investigated droplets impacting on substrates with various roughness and found that the critical impact We for splashing is a function of the ratio of the droplet radius to the surface roughness. Rioboo et al. [4] investigated the possible outcomes and parameter interactions for droplets impacting dry rigid surfaces. Their experiments also showed that waviness (waviness) suppresses detachment of satellite droplet. Josserand et al. [9] showed that an isolated obstacle can trigger detachment of satellite droplets. Latka et al. [10] found that surface waviness (waviness) inhibits splashing at maximum spreading.

Beside roughness and waviness of surfaces which are characteristic of fabrics, porosity and deformability of textiles may be important in droplet behavior. Thus, studying drop impact on porous and deformable surfaces can help us in determining their effect on textiles.

For identifying the effect of porosity, one can start by examining the basic principles of drop impact on one hole. Lorenceau and Quere [11] studied experimentally the behavior of a droplet (diameter, *D*, 1.5 to 3.5 mm) impacting at different velocities (0 to 3 m/s) on a stainless steel surface with a single hole (radius, *r*, 0.13 - 0.45 mm). They observed that at 0.5 m/s, *r*= 0.39 mm and *D*= 3.5 mm, droplet partially penetrated in the hole and no detachment of droplet on the opposite side of the hole, was observed (i.e. the liquid did not fully traverse the hole). In [11] a threshold velocity for liquid penetration (U^*) was given by balancing the dynamic pressure and the capillary pressure: $U^* \sim 2\sqrt{(\Upsilon/\rho r)}$;

(Υ is surface tension and ρ is liquid density), meaning the larger the radius of the hole, the lower the capillary pressure, and an easier droplet penetration. It can be understood that droplets with higher impact velocity penetrate easier on textiles with larger voids due to lower capillary pressure compared with dynamic pressure.

The closest systems to fabrics are meshes. Drop impact dynamics on meshes is similar to that of one hole; but, for meshes droplet will penetrate into many holes instead of one. Ryu et al. [12] studied drop impact on hydrophobic and super hydrophobic meshes, and found that the threshold velocity for penetration from [11] is valid for the meshes independent of their hydrophobicity. Soto et al. [13] Ryu's investigations and found that hole radius is a governing parameter in droplet penetration for meshes; the focus of this study was on droplet behavior after penetration and found that the larger the voids are, the larger the droplet ejection angles are [13]. It was understood that by increasing velocity, the angle of droplet ejection (the angle between mesh surface and speed direction) below holes will be increased. Boscariol et al. [14] attached a stainless steel surface below the meshes and compared droplet behavior with the one on a mesh with no substrate below. The difference is ejection of droplet from the mesh without any substrate below. It was demonstrated that when there is a substrate below the meshes, more energy will remain within the spreading droplet (droplets are penetrated in holes but not ejected or detached from the system). But, when there is no surface below a mesh, energy will be removed from the system by ejected droplets and droplet maximum diameter will be decreased.

One of the features of fabrics is their deformability. The effect of deformability on drop dynamics has been studied for soft non-porous surfaces. Pepper et al. [15] investigated the droplet behavior after impact on a stretchable polymer substrate. They changed the impact

velocity in the range of 1-3.5 m/s. They argued that splashing behavior of droplet is not change drastically with changes in membrane tension. But, they explained that elastic membrane converting some of the initial kinetic energy at impact to elastic energy. From the energy point of view, the elastic energy stored in a membrane is proportional to fabric tension.

Works that have been done in the area of drop impact on fabrics (which are porous surface) are very limited. Calvimontes et al. [16] studied the topography of fabrics and found that density of threads is responsible for the roughness of fabric. They found that by increasing warp and weft density, fabrics will be closer to the smooth surfaces and maximum spreading of droplet will be increased.

Romdhani et al. [17] found that weft count affects drop behavior (all of their experiments used a cotton plain woven fabric). They concluded that by increasing weft count droplet penetrate less in voids. Furthermore, they found that increase of weft counts results in an increase in the maximum spreading of droplet; but, it was not clear if the same behavior can be seen for other weaves. In a follow up study, Romdhani et al. [18] found that independent of the weave type, textiles with lower weft count possesses a loose structure and allow a higher level of drop penetration (Plain and Twill cotton weave were used). In both studies, Romdhani et al. [17,18] observed that after the droplet impact, the fabric will deform (so, it can be assumed there is no substrate below the fabrics), droplet spread gradually and eventually, it will penetrate in yarns and voids of fabrics. They have not mentioned tension in fabrics and did not talk about the effect of waviness (undulation) on droplet behavior.

Despite these studies, questions still remain about drop impact on fabrics. The effect of droplet penetration on fabrics spreading phase is still questionable; it is not clear that how much energy will be removed from the system by penetration. Energy analysis is important due to its direct effect on maximum spreading of droplet. Besides, it is not clear that how much energy will be consumed for fabric deformation and if this amount can affect dynamics of droplet or not. Also, no study has been done on the effect of waviness of fabrics on dynamics of droplet in spreading phase. Also, there is no model to predict droplet behavior on fabrics.

Due to importance and lack of investigation on drop impact on fabrics, it is necessary to study drop impact on fabrics to identify parameters that can affect droplet behavior. Besides, this study can be used for changing fabrics structure in clothing industry for make clothes water repellant. As it was mentioned wettability of surfaces are important in drop impact; but, used fabrics in this are all made from the same material (polyester) that make their wettability the same. Thus, wettability is not investigated in this study. Five different woven type fabrics (in other words different topography) are used to understand effect of porosity, waviness and flexibility of fabrics in droplet behavior. The reason for choosing mentioned five fabrics is due to their high usage in clothing industry. Then, droplet behavior is investigated at different impact velocities and tensions on all fabrics which is the first goal of this study. Also, as a base case, drop behavior on polyester coated glass has been compared with the ones on fabrics to clarify effect of fabric topography on dynamics of droplet. Physical interpretation is suggested for droplet in each case. At last, a model that can predict droplet behavior on fabrics is introduced and has been validated by experimental results.

Chapter II: Theoretical Model Development

In this chapter, the theoretical model used to investigate the dynamics of drop impact on various fabrics, is introduced.

2.1 Energy-based model

To study droplet behavior on fabrics, a model based on “energy balance” is developed. Analysis is done between two moments: the moment of impact and the moment of maximum spreading of droplet. This equation can be written between the impact time and any moment while spreading and droplet kinetic energy should be considered at any moment; knowing the maximum surface coverage that an impacting drop can reach is of great importance in a wide variety of applications like ink-jet printing, spray cooling and blood spatter analysis [36]. See Figure 2.1.

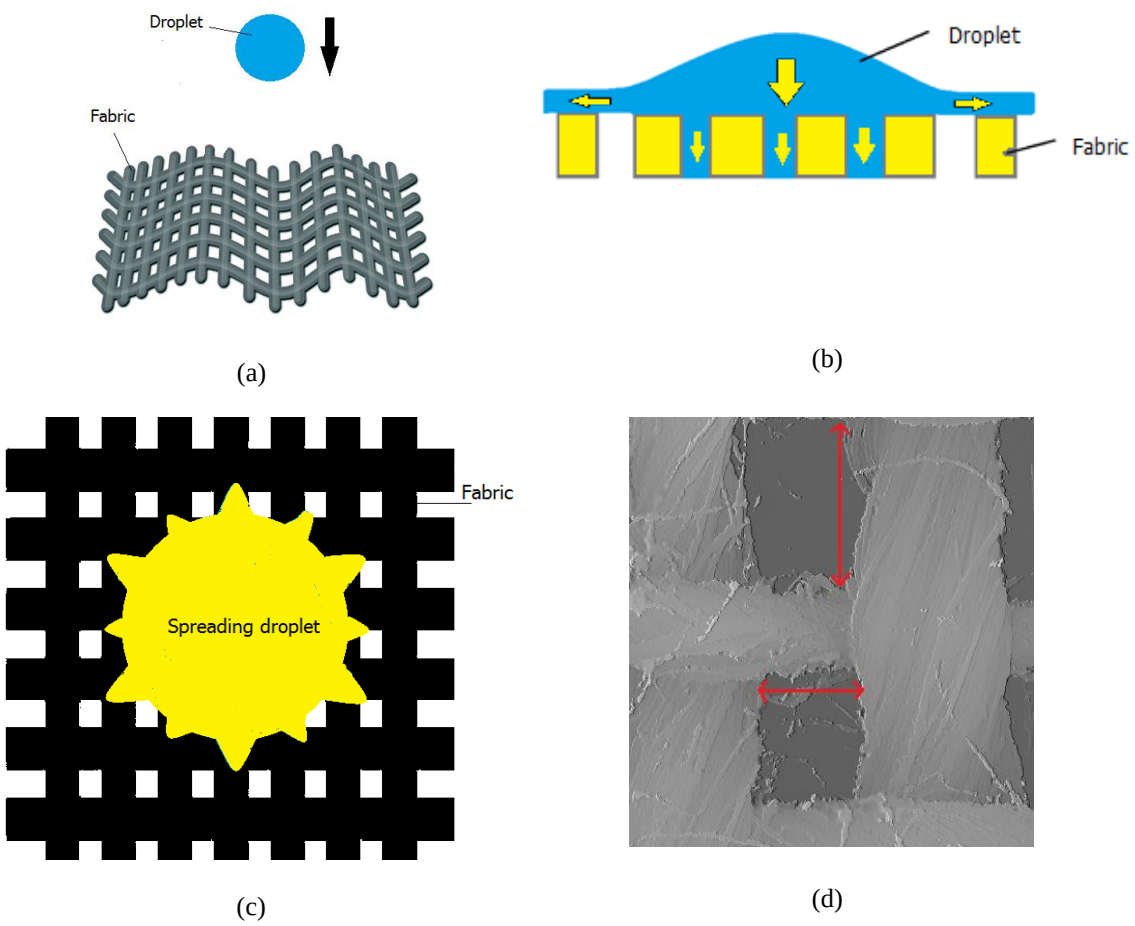

Figure 2.1: a) Schematic view of droplet before impact. b) Side view of droplet impact at maximum spreading. c) Top view of droplet impact at maximum spreading. d) microscopic view of fabric voids

In introducing a model for droplet impact, the classical approaches encounter two problems with the prescription of boundary conditions at the triple contact line [19]. First, a shear-stress singularity is implied by the no-slip condition at the wall when droplet spread after impact. Second, the static contact angle (contact angle with which the contact area between liquid and solid is not changed from the outside during the measurement) depends on the material property while the dynamic contact angle is not. Considering this last point, it is often suggested to identify the difference between an apparent dynamic contact angle

(contact angle which is produced in the course of wetting or de-wetting) and a real dynamic contact angle. Whereas the former is the one obtained by traditional experimental means or simulations, the second is considered to be experimentally inaccessible at the molecular scale at the wall. Thus, an empirical model considering this inner dynamic contact angle as a function of triple line velocity and static contact angle is introduced when a droplet impact on surfaces [20]. In contrast with most of these approaches, Blake et al. [21], found that the failure to describe the relation between the contact angle and the flow field in spreading droplet is a major problem in the common used models in drop impact area.

In an effort to make connection between contact angle and the flow field, Shikhmurzaev [22] introduced a self-consistent model of the contact-line motion for spreading droplet after impact. Along with describing flow behavior, the model introduces a definition of the surface tension gradient near the moving contact line. They consider the hydrodynamics of the liquid-liquid displacement, i.e. the flow on length scales large compared with the interfacial layer thickness over the actual surface of a solid. This gradient is appeared because of the process by which the liquid-gas interface is replaced by the liquid-solid interface forms as the droplet spread on the wall. While this model was able to fit experimental data of drop spreading phase in the quasistatic regime, it could not describe the initial spreading phase. Such analytical solutions that used simplifying assumptions were not applicable to the initial phase of spreading droplet where none of the inertia, dissipation, and surface tension effects are negligible. In the following, the concentration changed to numerical solutions of the Navier-Stokes equations and on approximate one dimensional models were introduced for the spreading phase of droplet.

To allow the contact line to slip while spreading and to fix the dynamic contact angle, Fukai et al. [23] used deforming finite elements. Renardy et al. [24] used a free-slip condition with a specific dynamic contact angle to model the drop spreading after impact on super-hydrophobic surfaces. To omit the need for considering a slip condition, Pasandideh-Fard et al. [25] used a method based on the concept of a fractional volume of fluid. They considered the specific dynamic contact angle as a boundary condition based on their experiments. Using experimentally determined dynamic contact angles prevent a predictive use of all mentioned models. Sikalo et al. [26] used a better approach by using volume of fraction method based on the Cox model [27] with a predictive empirical correlation giving the dynamic contact angle as a function of velocity at the triple line while droplet spreading. Although, there are some doubts regarding the usage of such correlation to predict dynamic contact angle in droplet spreading phase after impact, the numerical model of Sikalo et al. [26] describes the spreading and receding contact angle of the drop as well. In all of the mentioned models, the main deficiency is the lack of self-consistency between the description of kinetic energy and viscous dissipation which is solved in the model used in this study; but, the introduced model in this study has solved all mentioned problems.

The scope of introduced model is to predict maximum diameter of droplet after drops impact on fabrics which all have the same material (polyester). Besides, the effect of factors like deformation and penetration, which are fabric features can be analyzed. This model is written between the impact time and the time in which droplet reaches maximum spreading. It will be discussed in next chapters that some factors will be negligible compare to other factors.

Equation 2.1 shows the energy balance between the moments of impact (left-hand side) and maximum spreading of droplet (right-hand side).

$$E_{S1} + E_{k1} = E_P + E_e + E_v + E_{S2} \quad (2.1)$$

E_{S1} is the initial surface energy, E_{k1} is the initial kinetic energy of droplet, E_P is energy removed due to droplet liquid penetrating through voids, E_e is the elastic energy stored in the fabrics, E_v is the viscous dissipation energy, and E_{S2} is the surface energy of the lamella at maximum spreading. In the following, each parameter in Equation 2.1 is separately calculated.

2.1.1 Initial Surface Energy (E_{S1})

Initial surface energy of droplet is calculated by multiplication of surface tension and surface area of droplet. Thus, it is only a function of droplet diameter, droplet liquid and environment temperature which are constant the same in our experiments.

2.1.2 Initial Kinetic Energy (E_{k1})

Knowing the initial impact velocities (U) of droplet, the corresponding kinetic energy for each different velocity is calculated. It is obvious that by increasing velocity, initial kinetic energy of droplet will be increased.

2.1.3 Penetration Energy (E_P)

During drop impact, some part of the droplet may directly penetrate through the voids of the fabric and therefore, will not participate in spreading of the droplet. This can be equated to loss in total energy of the droplet, which is called penetration Energy.

2.1.4 Elastic Energy (E_e)

Elastic energy is the mechanical potential energy stored in the configuration of a material or physical system as it is subjected to elastic deformation by work performed upon it. When the droplet impacts a flexible surface, the surface will be deformed. Thus, some part of the kinetic energy of droplet will be transformed to elastic energy.

2.1.5 Viscous Dissipation Energy (E_v)

It is necessary to clarify the difference between surface roughness and surface waviness, in order to discuss the energy dissipation due to surface waviness. The importance of this difference is that, waviness increases the area on which viscous dissipation happen and directly affect the amount of viscous dissipation. In the literature, the emphasis has been on surface roughness and its impact on splashing and spreading in drop impact phenomenon. However, for surfaces such as fabrics, surface waviness plays a separate role as that of surface roughness as explained below. It has been found that depending on how topography of surface is measured (for example at different cut-off length which is the length of fabrics when taking measurements), variations in interfacial energies will be found [28].

Surface roughness is a component of surface texture. It is quantified by the deviations in the direction of the normal vector of a real surface from its ideal form. If these deviations are large, the surface is rough; if they are small, the surface is smooth.

Surface waviness is the measurement of the more widely spaced component of surface texture and it is a broader view of surface topography. In other words, waviness is the quality of curving back and forth on the surface. Waviness of fabrics in this study are in the order of 0.1mm and the roughness is in the order of 0.001mm. Figure 2.2 shows the difference between roughness and waviness.

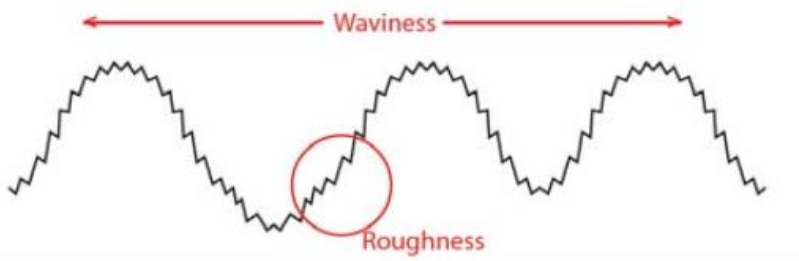

Figure 2.2: Schematic of difference between roughness and waviness

During spreading of a droplet on different surfaces, some part of total energy of droplet will be dissipated through viscous forces which is called viscous dissipation energy (E_v).

Chapter III: Method and Materials of the Experiments

In this chapter, the method of our experiments and the experimental setup used for experiments, are explained in detail.

3.1 Fabrics used

Polyester fabrics of different weaving types: Satin, Warp knit, Mesh, Plain and Weft weave, were used in the experiments. Polyester is the most usable material for fabrics. A schematic of their structures is displayed in Figure 3.1.

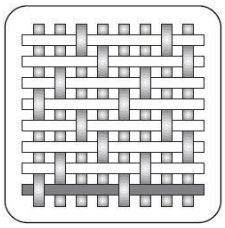

Satin weave

Warp knit

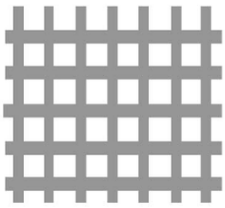

Mesh weave

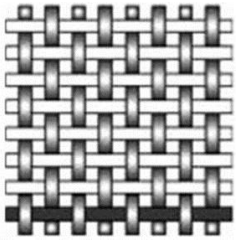

Plain weave

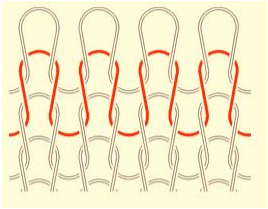

Weft knit

Figure 3.1: Schematic view of Fabrics with five different weaving types [44].

The reason that these five types of fabrics are used in our experiments is that, in clothing industry the usage of these 5 weaves is mainly common. The reason that weaving type is important is that, weaving type result in different features of fabrics such as deformability, waviness, void size, etc.

Although there are different materials which are used in textile industry, the material of all fabrics in this study are polyester; because polyester has the vast usage (up to 70%) in clothing industry.

3.2 Method and Setup

In our experiments, droplets with a diameter of 3mm were used. This diameter is chosen randomly and final calculation is independent from droplet size. The droplet liquid was water due to higher exposure of clothes to water compare to other liquids. Test were done at room temperature i.e. 23^0 C. Droplets were generated with the syringe on top of the fabrics; then, droplets released on fabrics with different impact velocities (see Appendix H).

Table 3.1: Droplet impact velocity (2% error) and We number at the impact point

Impact velocity (m/s)	We Number
1.45	93
5	165
2.5	256
3	371

Velocities were changed by adjusting distance between needle that generate the droplets and fabrics. Fabric samples had a rectangular shape (6 x 6 cm^2); three different tensions using forces of 0.23 N, 1.07 N and 1.6 N, were applied to each of the four sides of fabric samples. These forces are applied on fabrics by hanging four metal rods from four side of fabrics shown in Figure 3.2.

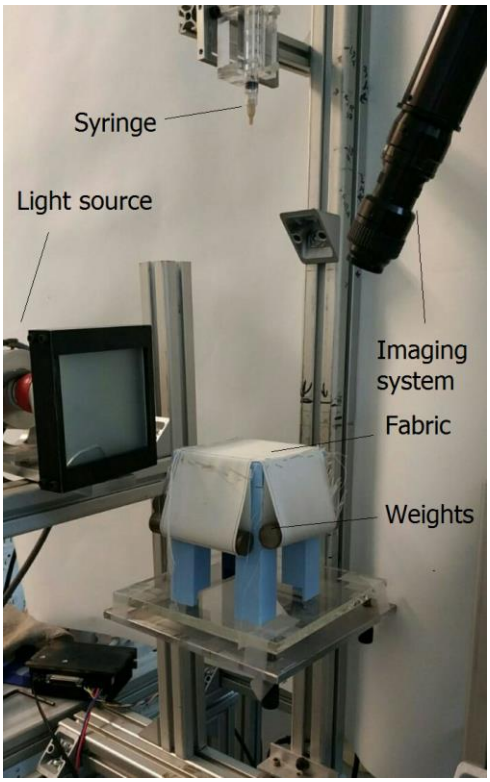

(a)

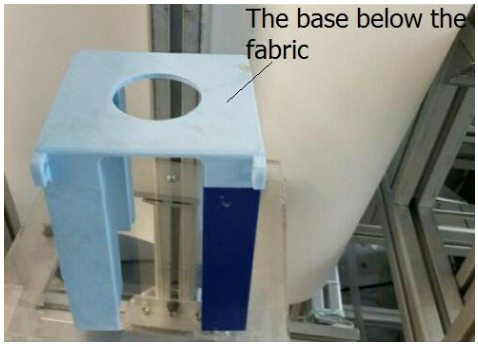

(b)

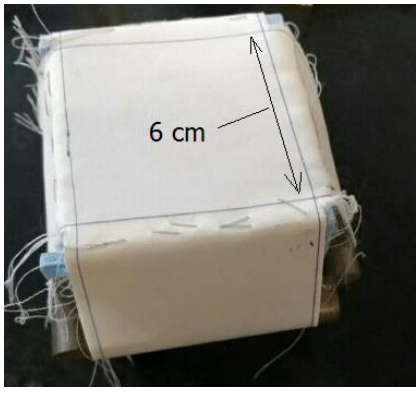

(c)

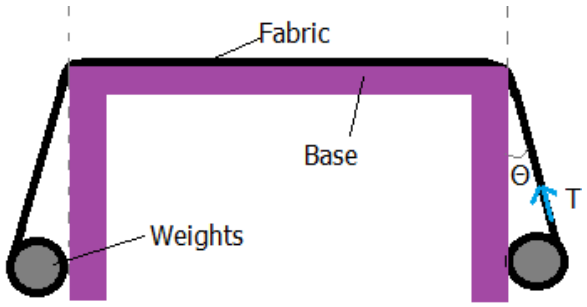

(d)

Figure 3.2: Drop impact setup from a. Side view. b. the base below the fabric. c. the top view of fabric. d. Schematic of setup, weights and fabric tension

It is noteworthy that the **angle** between the weights and the base has been neglected due to its low amount (see Appendix H). Thus, it is reasonable to consider the tension vertically

in the calculations. As it is shown in Figure 3.2, just one top view camera was used as a side view camera is not usable (because of the deformability of fabrics and due to vertical movement of droplet, it will become invisible to the side view camera). Controlling impact velocity and measurements with high speed camera will result in errors which are shown in results chapter. In order to decrease these errors, each experiment was repeated three times. As it is shown in Figure 3.2, one base with a hole on top of that is placed below the fabric. The usage of this hole is to meet the condition that no surface should be below the fabric. Thus, when the droplet impact on fabrics, it is in contact just with fabrics. After droplets released from the syringe of fabrics, the Phantom V 340 high speed camera starts to record droplet behavior from top view. This recording continue till the droplet settles on fabrics with no movement. Also, a light source has been located on one side of fabrics to make the surface of fabric bright while recording which is shown in Figure 3.2.

Regarding the tensions which are applied on four sides of fabrics, in open literature, there is no information about tension on fabrics when worm on a clothing; but, it is known that when producing shirts, sewing machines exert a maximum force of 7 N to threads [29]. In their experiment thread tension is imposed to a device called tensioner and they started to exert force from 0 to 7 N. They found that the maximum force that can be applied to thread was 7 N. It was shown that after larger forces result in tearing of threads or the thread will be entered in the plastic region (pass its elastic limit). To omit the wettability effect of surface beneath the fabric, underneath the fabric was exposed to air and no substrate was placed under the fabric (around the drop impact point).

To isolate the effect of wettability from the texture of fabrics, droplet impact on polyester coated glasses was tested which is the same material of fabrics. This coating can be an

appropriate representative for fabrics material. For coating glass, 1 wt% solution of polystyrene in toluene was used to coat the glass; then, the mixture is used to coat the surface with the spin-coater with spin-velocity of 1200 rev/min.

For finding dimension of voids in a fabric, the fabrics were examined by a sensofar optical microscope under different tensions. For each fabric type, shapes of voids are different, and sometimes irregular. We fitted specific shapes to voids in each fabric e.g. circle (for Mesh woven), rectangle (Plain woven) and triangle (Warp and Weft knit). Then, area of voids was calculated by measuring the dimensions of voids and finding their approximate area. Then, the diameter of an equivalent circle having the same area as voids was obtained, to represent the void size for each fabric type.

To measure the amount of fabric deflection, first, we considered a point 4 mm away from the impact point which is named A in Figure 3.3 (we chose this distance based on the maximum spreading of droplets). For measuring the deflection of fabric at the impact point, we should note that the diameter of the hole below fabric is 4 cm. It is obvious that fabric deflection at the perimeter of this hole is zero (point c). Thus, by trigonometry, deflection of fabric at the impact point will be derived easily. It is noteworthy that due to low amount of deflections, it is assumed that fabric movement from point c to impact point changes linearly (fabric deflection changes is linear at the impact moment. Because at the impact moment one force directly is applied to one point vertically to the fabric).

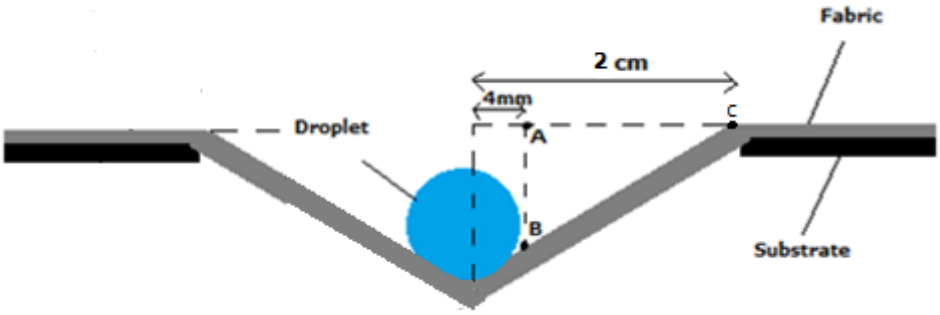

Figure 3.3: Fabric at its maximum deflection. Fabric is shown pointy for better understanding of deflection measurement

The amount of movement was found by capturing images before impact and at maximum deflection and then measuring distance between these two points which are named A and B in Figure 3.3 (in another words, B is the maximum deflection and A is the initial location of B before impact).

Splashing and finger formation is seen (mainly for We of 256 and 371 for all fabrics which are shown in Table 4.1); thus, maximum diameter of droplet cannot be measured directly. As a result, the distance between the center of impact and different points of droplet (fingers and the space between fingers) were measured by a scale. Then, the average of these distances was considered as a proxy for maximum spreading diameter of droplet.

Chapter IV: Experimental Results

Droplets are released from different heights on fabrics under different tensions and droplets behavior is recorded by high speed camera. Images at maximum spreading of droplet and after spreading are captured from recorded videos. Maximum diameter and time for reaching that has been measured for comparison between different velocities and tensions. Tables 4.1 to 4.5 show the droplet at its maximum spreading and after recoiling in different impact velocities and fabric tension. Time for reaching maximum diameter of droplet is shown in each case (images are not at the same time and they are just at their maximum diameter). In cases that droplet boundary is not clear (because of the color of the fabrics), additional lines are used to show the boundary clearly. Initial impact velocities (U) of droplet are 1.45 m/s, 2m/s, 2.5 m/s and 3 m/s, which correspond to a kinetic energy of 14.8 μJ, 21.6 μJ, 34.1 μJ and 57.5 μJ, respectively. All experiments have been done for three times. At each time, all parameters like impact velocity, droplet diameter, maximum spreading, etc. has been measured and their average has been considered as the amount for each parameter. It is obvious that the discrepancy between measured parameters is considered as the error for all measurements and calculations (see Appendix A and H).

Table 4.1: Drop impact on satin weave at different impact velocities and fabric tensions including time for maximum spreading of droplet (4%-time error)

Tension / We Num.	0.23 N	1.07 N	1.6 N
We= 371	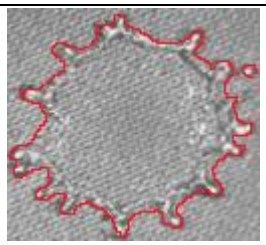 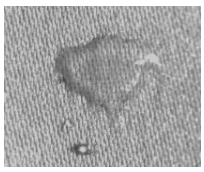 5mm t max= 3250 µs	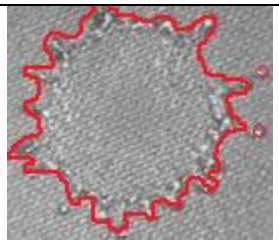 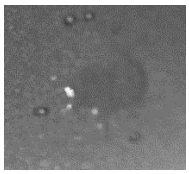 5mm t max= 3150 µs (-7 %)	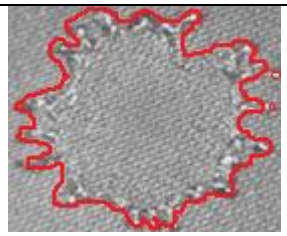 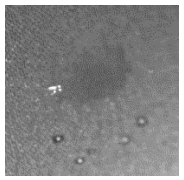 5mm t max= 3050 µs (-13%)
We= 256	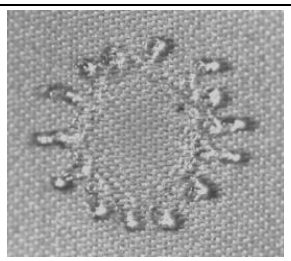 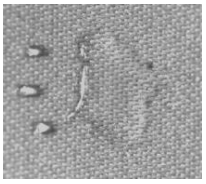 5mm t max= 3300 µs	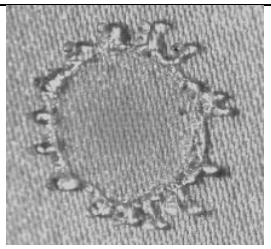 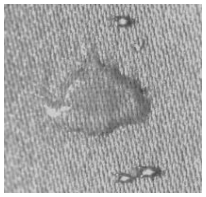 5mm t max= 3250 µs (-16 %)	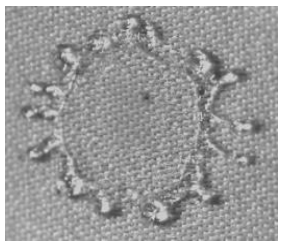 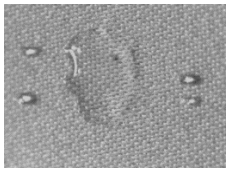 5mm t max= 3220 µs (-25.24%)

We= 165	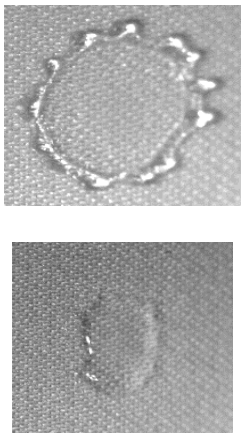 t max= 3475μs	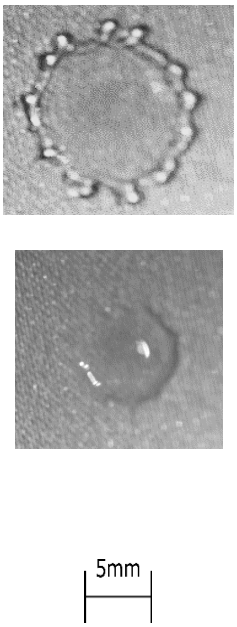 t max= 3320 μs (-21 %)	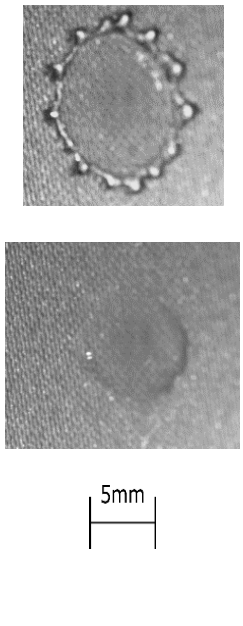 t max= 3250 μs (-25 %)
We= 93	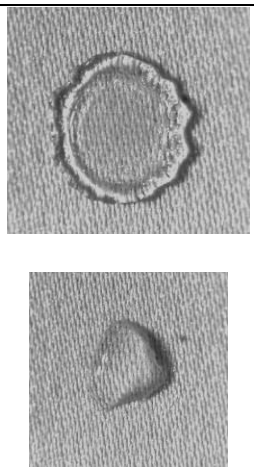 t max= 3550 μs	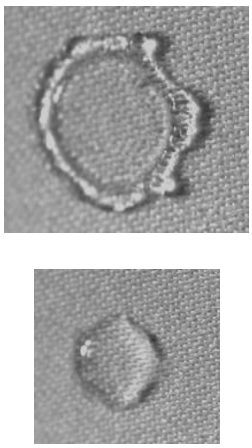 t max= 3450 μs (-4 %)	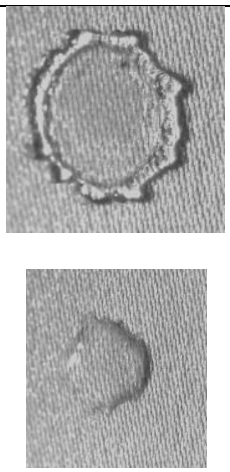 t max= 3365 μs (-8.6 %)

Table 4.2: Drop impact on warp knit at different impact velocities and fabric tensions including time for maximum spreading of droplet (4% time error)

Tension / We Num.	0.23 N	1.07 N	1.6 N
We= 371	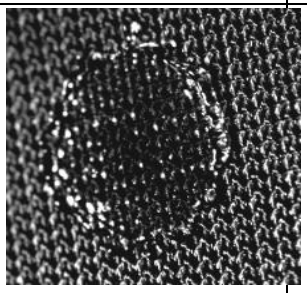 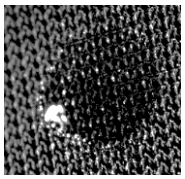  5mm t max= 3050 µs	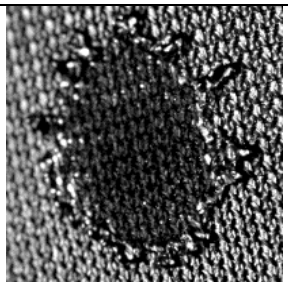 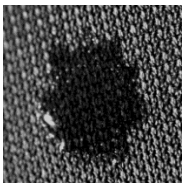  5mm t max= 3000 µs (-8.6%)	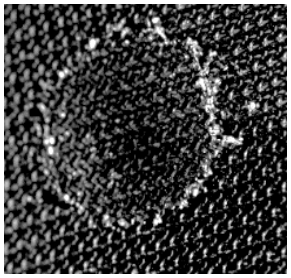 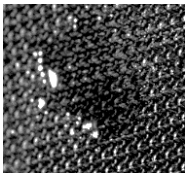  5mm t max= 2950 µs (-14.6)
We= 256	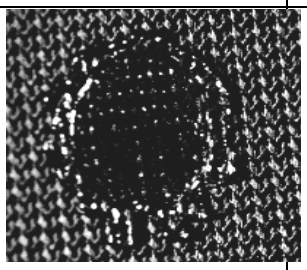 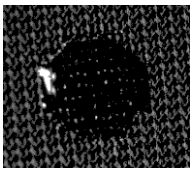  5mm t max= 3200 µs	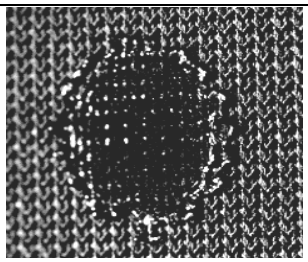 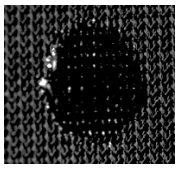  5mm t max= 3100 µs (- 7%)	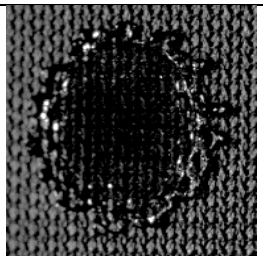 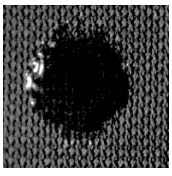  5mm t max= 3050 µs (-13.3 %)

We= 165	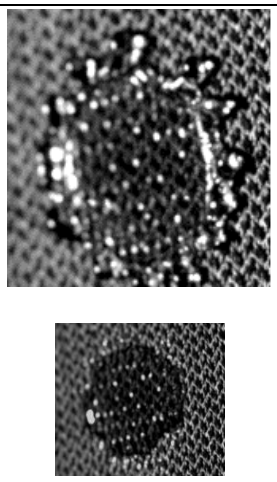 t max= 3300 µs	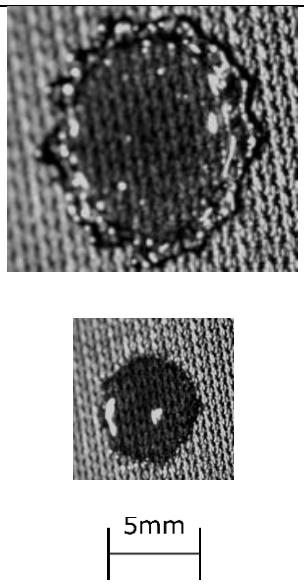 t max= 3200 µs (-8.2 %)	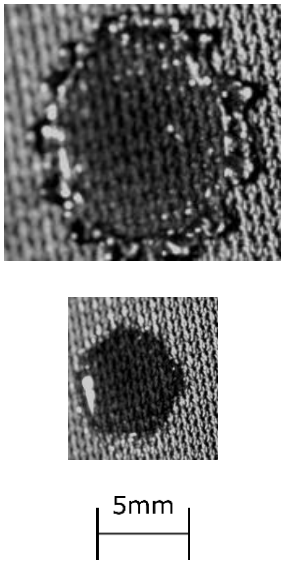 t max= 3100 µs (-13.34)
We= 93	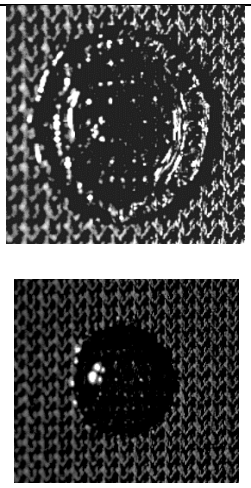 t max= 3540 µs	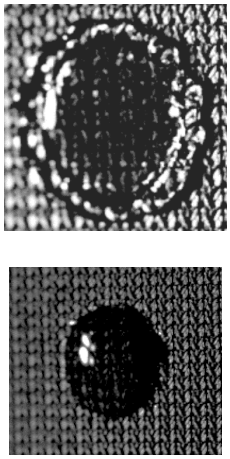 t max= 3250 µs (- 5%)	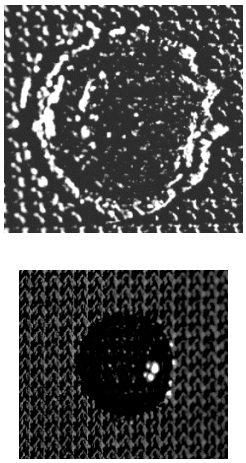 t max= 3200 µs (-9 %)

One of the important observations that can be found in Tables 4.1 to 4.5 is that increasing tension does not affect droplet behavior drastically. In other words, the only difference in droplet behavior at different tension is the time for reaching the maximum diameter of

droplet. This can be due to the fact that tensions in the experiments are not large enough to change droplet behavior (it will be discussed in next chapter).

As it is shown in Tables 4.1 to 4.5, when the droplet impact on fabrics with different weaving types, its behavior and time for reaching maximum diameter will differ. Also, We number affect droplet behavior drastically and it changes droplet spreading shape from circular spreading to flower shape spreading (splashing).

Table 4.3: Drop impact on weft knit at different impact velocities and fabric tensions including time for maximum spreading of droplet (4%-time error)

Tension / We Num.	0.23 N	1.07 N	1.6 N
We= 371	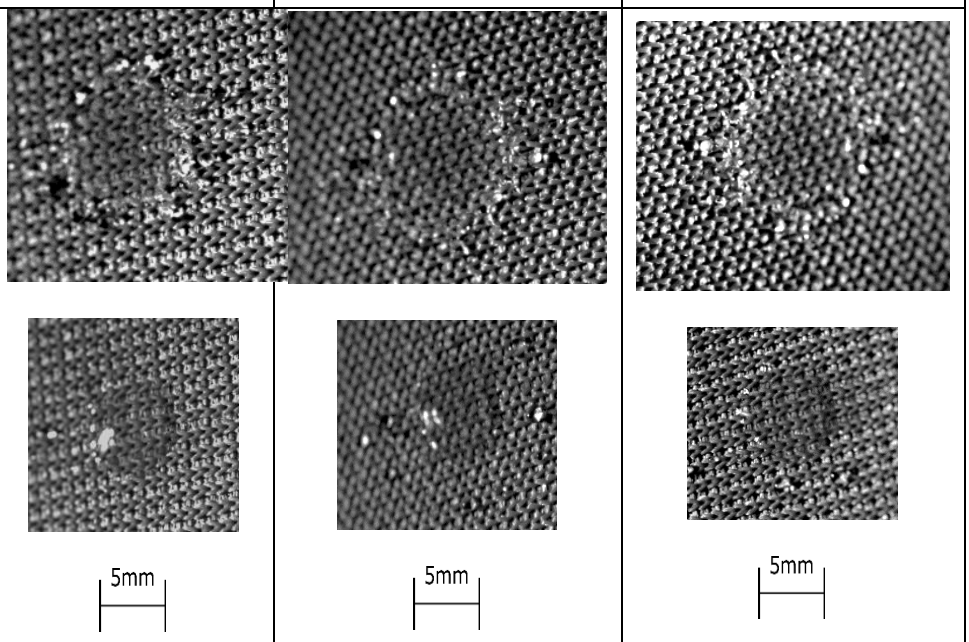	t max= 3050 µs	t max= 2950 µs (-7.12 %)	t max= 2900 µs (-12.4 %)
We= 256	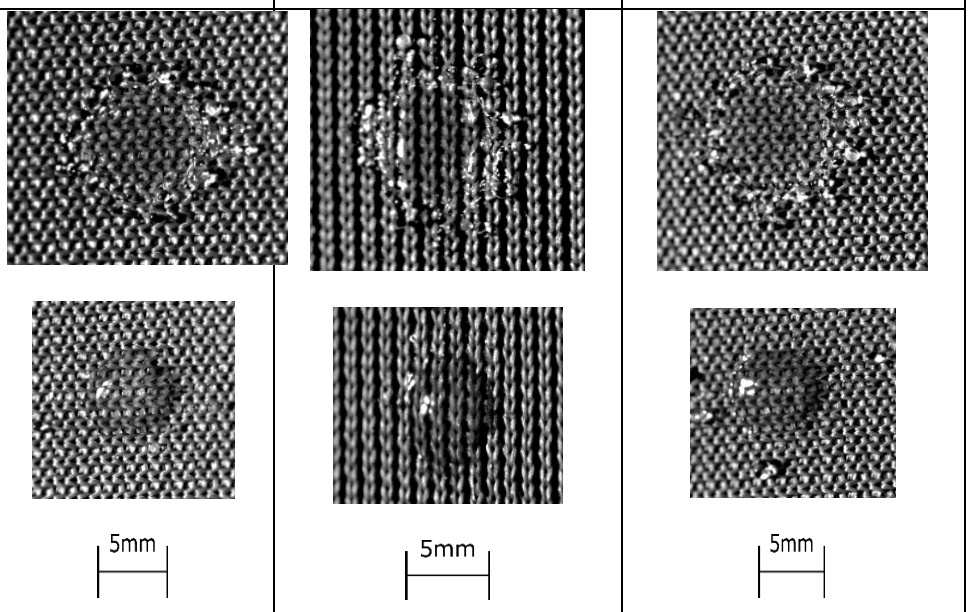	t max= 3200 µs	t max= 3050 µs (-6.22 %)	t max= 2950 µs (-10 %)

We= 165	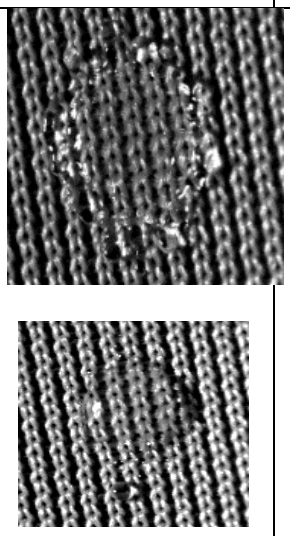 t max= 3350 µs	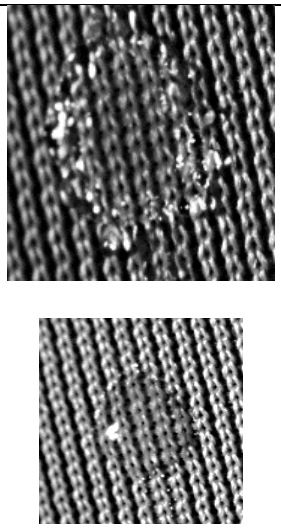 t max= 3250 µs (-6.6 %)	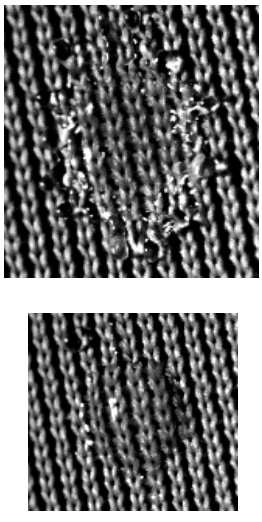 t max= 3150 µs (-12.7)
We= 93	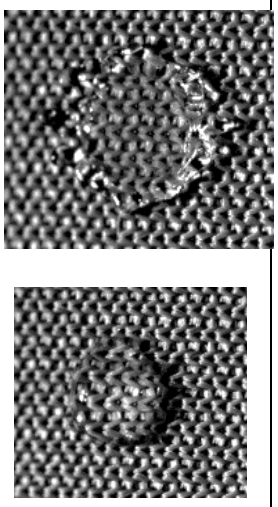 t max= 3450 µs	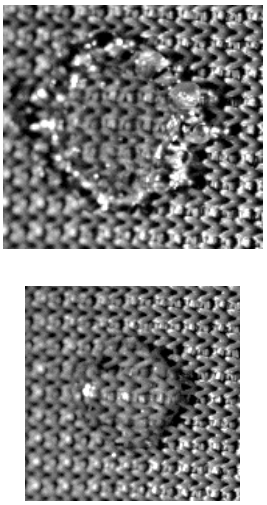 t max= 3400 µs (-5.8 %)	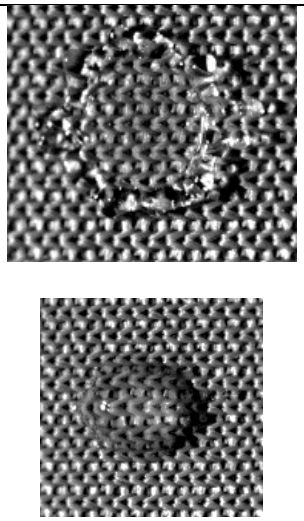 t max= 3250 µs (-9.5 %)

It is noteworthy that by increasing velocity, droplet reaches sooner to its maximum spreading, and time for reaching maximum diameter will be decreased. Besides, increasing tension result in faster spreading of droplet; this can be due to lower deflection energy (E_d) which is stored in the fabric that lets spreading droplet to spread with higher kinetic energy (it will be discussed completely in next chapter).

Table 4.4: Drop impact on plain weave at different impact velocities and fabric tensions including time for maximum spreading of droplet (4%-time error)

Tension / We Num.	0.23 N	1.07 N	1.6 N
We= 371	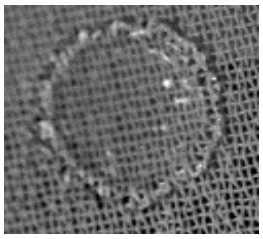 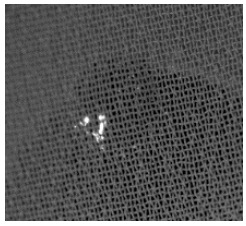  t max= 2850 µs	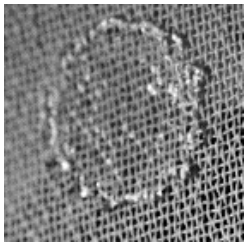 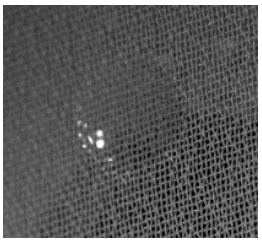  t max= 2750 µs (-5.4 %)	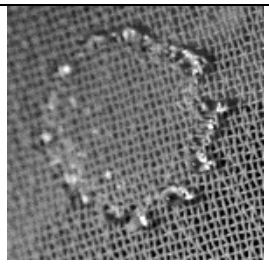 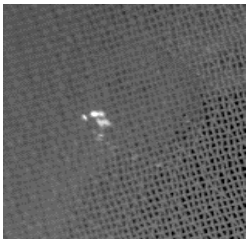  t max= 2700 µs (-8.7 %)
We= 256	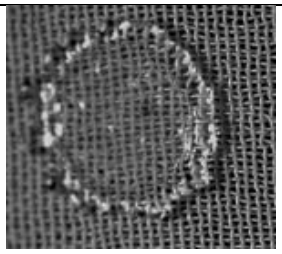 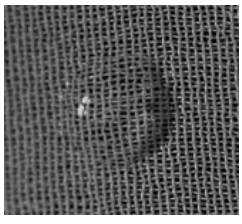  t max= 3050 µs	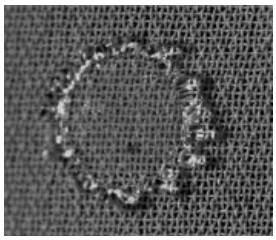 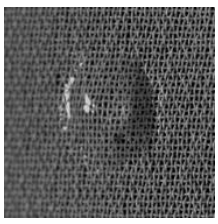  t max= 2950 µs (-7 %)	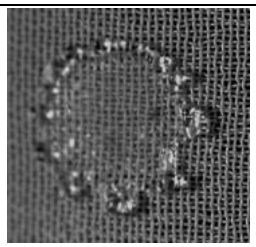 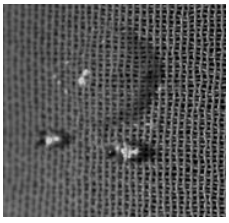  t max= 2850 µs (-11.11 %)

We= 165	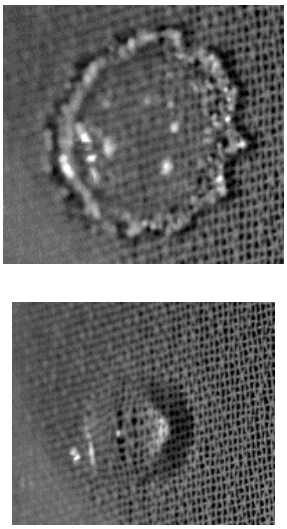 t max= 3150 µs	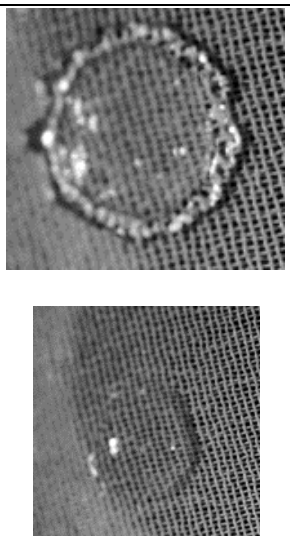 t max= 2950 µs (-6.7 %)	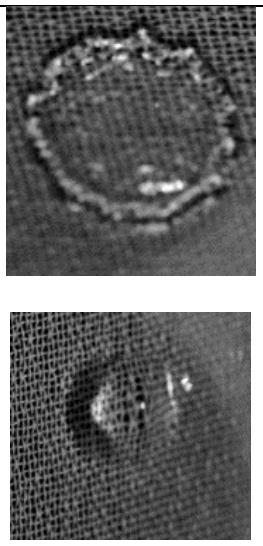 t max= 2850 µs (-10.6 %)
We= 93	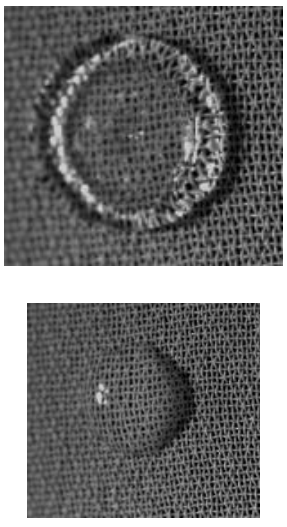 t max= 3300 µs	 t max= 3200 µs (-6.3 %)	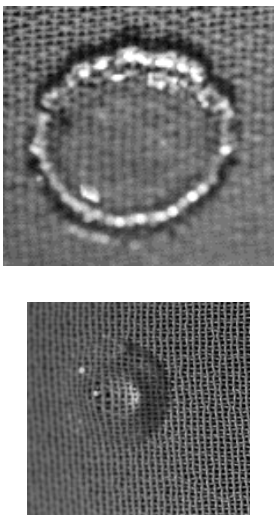 t max= 3150 µs (-11.32 %)

Table 4.5: Drop impact on mesh weave at different impact velocities and fabric tensions including time for maximum spreading of droplet (4%-time error)

Tension / We Num.	0.23 N	1.07 N	1.6 N
We= 371	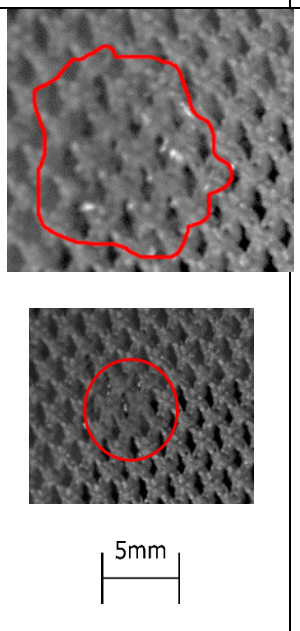 t max= 2800 µs	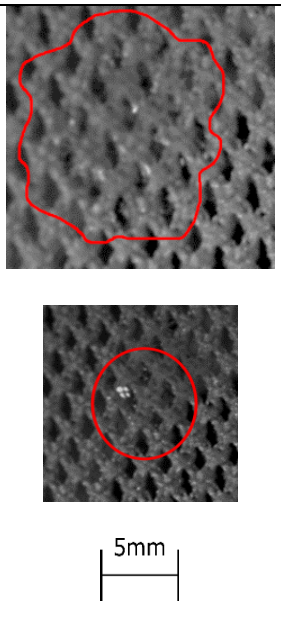 t max= 2750 µs (-3.8 %)	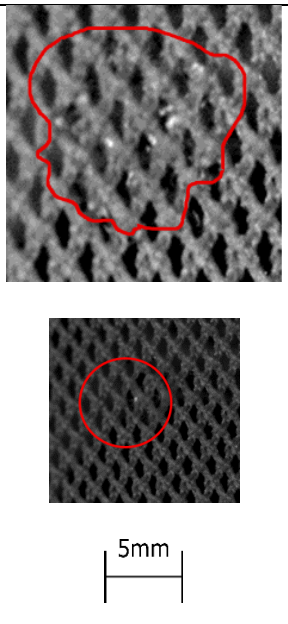 t max= 2700 µs (-5.4 %)
We= 256	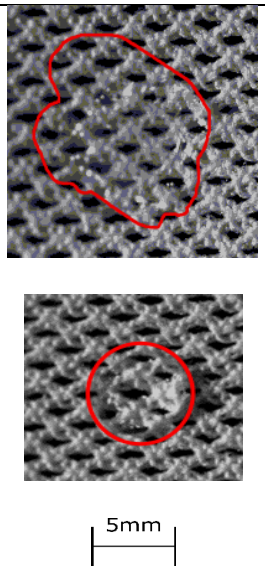 t max= 2925 µs	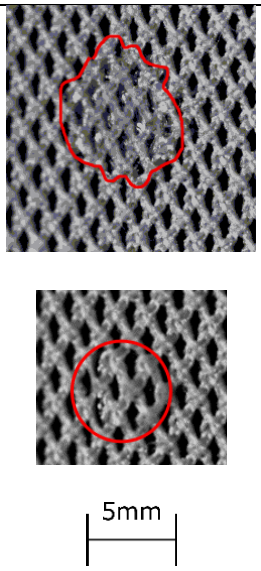 t max= 2800 µs (-2.8 %)	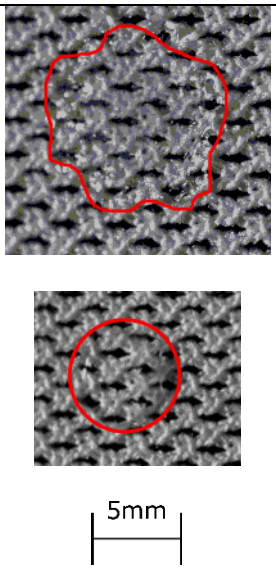 t max= 2750 µs (- 4.8 %)

We= 165	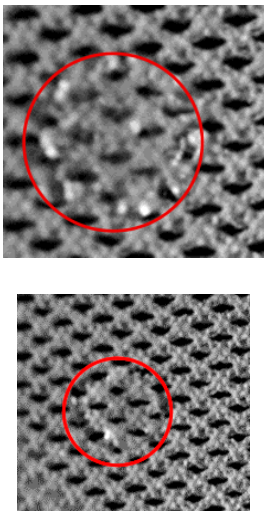 t max= 3050 µs	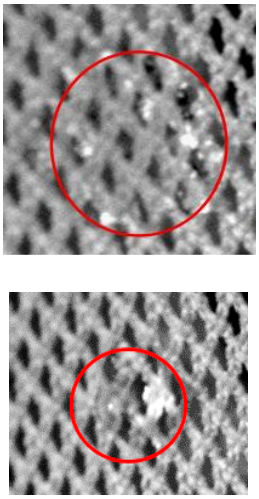 t max= 2950 µs (-6 %)	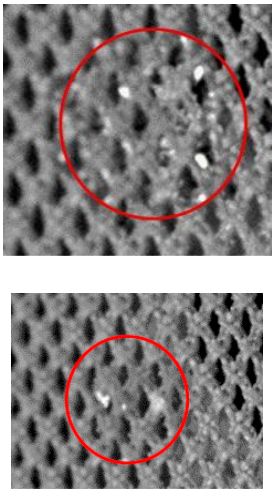 t max= 2900 µs (-7.6 %)
We= 93	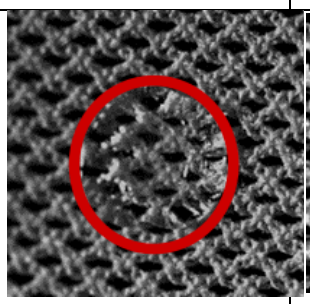 t max= 3250 µs	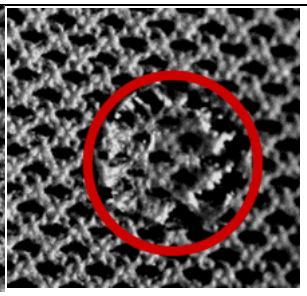 t max= 3150 µs (-5 %)	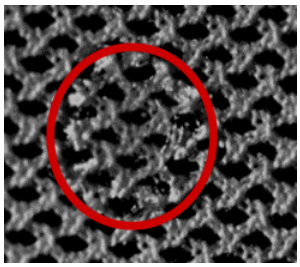 t max= 3050 µs (-9.3 %)

Table 4.6 shows droplet maximum spreading after impact on a polyester coated glass (images are not at the same time and they are just at their maximum diameter).

Table 4.6: Top view of droplet impact on glass surfaces coated with polyester (4%-time error)

	 t_{max}= 3000 µs	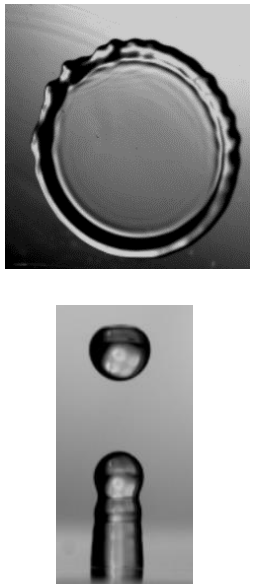 t_{max}= 2850 µs	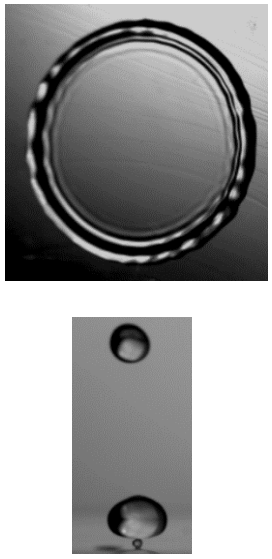 t_{max}= 2750 µs	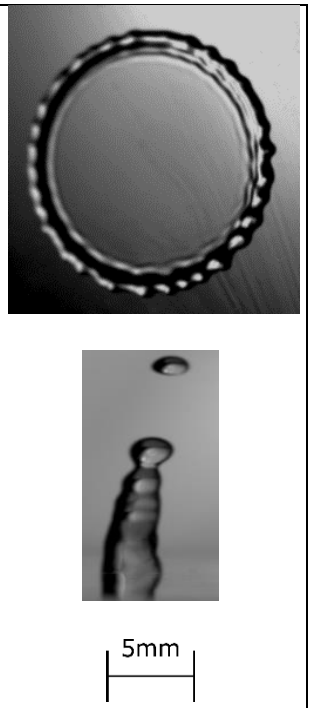 t_{max}= 2700 µs
We Num.	93	165	256	371

Using the method explained in 2.1.1, at temperature of 23 ^{o}C, the surface energy of droplet is 2.05 µJ (see Appendix A).

Chapter V: Interpretation of Experimental results

In this chapter, the results of our experiments and the calculated results of our model are compared, physical interpretation of the results are presented and validity of our model is established. Besides, it is tried to simplify the model introduced in this study by omitting factors which their values are negligible compare to the total energy of droplet.

Apart from calculations, it can be understood from observations in previous chapter that, deflection energy would be negligible due to similar behavior of droplet at different tensions. Also, increasing tension will not change void size and E_p due to similar behavior of droplet at different tensions; but, at higher value of tensions droplet void size will be changed that increase droplet penetration. Besides, observing increase in diameter of droplet at higher velocity would be due to the fact that most of the initial energy of droplet may be transformed to surface energy.

5.1 Penetration Energy Results

5.1.1 Physical Interpretation

Studying penetration is essential for drop impact on porous surfaces. When droplet impact takes place on a porous surface, it imparts vertical momentum downward through voids. Thus, some part of droplet liquid may penetrate into voids and will not take part in spreading of droplet [12]. Based on previous works about drop impact on porous surfaces [11,12,30], drop penetration into voids will not be possible, unless dynamic pressure is higher than capillary pressure. As mentioned in these studies, during drop penetration,

some energy is removed from system by penetrated liquid through voids. Therefore, it can be assumed that some part of the total energy of droplet will be lost (E_P) after impact on fabric by penetration. As a result, less energy remains for the spreading phase of droplet, which may cause a decrease in its maximum spreading.

5.1.2 Calculation

For penetration of droplets into the voids, dynamic pressure (P_D) should be larger than the capillary pressure (P_C). Capillary pressure ($\gamma.\Gamma/A$) is a function of surface tension (γ) of droplet and the size of voids. Here A and Γ represent the opening area of voids ($\approx r^2$) and perimeter of voids ($\approx 4r$); r is the radius of pore. Dynamic pressure is equal to ½. $\rho U^2 c$ (ρ is the liquid density)**;** in which "c" (scale factor) is a function of effective area. The scale factor (c) is found by balancing $\rho c U^2$ and $\gamma\Gamma/A$ for drop impact on meshes with different void sizes. For hydrophobic meshes, c is 2.78 [12]. In our work, due to the similar capillary pressure, range of void area, and wettability of fabric, we can consider 2.78 due to the same experimental systems.

Table 5.1 shows changes in the average area $(\mu m)^2$ of voids and capillary pressure (Pa) including percentage of changes, with different tensions for fabrics used in this study (see Appendix H).

Table 5.1: Average area of voids and capillary pressure of fabrics with different tensions (including percentage of changes in capillary pressure; errors is 4 %)

Tension / Weaving	0 N	0.23 N	1.07 N	1.60 N
Satin weave	0 $(\mu m)^2$	0 $(\mu m)^2$	0 $(\mu m)^2$	0 $(\mu m)^2$
Warp knit	19,200 $(\mu m)^2$	19,520 $(\mu m)^2$ 517 Pa	20,000 $(\mu m)^2$ 509 Pa (-1.5 %)	20,100 $(\mu m)^2$ 507 Pa (-1.9 %)
Weft weave	22,330 $(\mu m)^2$	22,550 $(\mu m)^2$ 479 Pa	23,100 $(\mu m)^2$ 473 Pa (-1.2 %)	23,200 $(\mu m)^2$ 472 Pa (-1.4 %)
Plain weave	29,710 $(\mu m)^2$	29,900 $(\mu m)^2$ 416 Pa	30,760 $(\mu m)^2$ 410 Pa (-1.4 %)	30,920 $(\mu m)^2$ 409 Pa (-1.7 %)
Mesh weave	190,520 $(\mu m)^2$	190,750 $(\mu m)^2$ 165 Pa	197,640 $(\mu m)^2$ 162 Pa (-1.8 %)	199,130 $(\mu m)^2$ 161 Pa (-2.4 %)

Dynamic pressure of droplet in the moment of impact at 1.45 m/s, 2 m/s, 2.5 m/s and 3 m/s will be 3,127.5 Pa, 5,560 Pa, 8,687.5 Pa and 12,510 Pa, respectively. In Satin weave, fabric threads are interconnected and there is no void. But generally for other fabrics, by increasing tension, void areas are increased, which results in a decrease in capillary pressure. Comparing the dynamic pressure values with capillary pressures in Table 5.1, one predicts that liquid will penetrate into voids.

By evaluating the results of Table 5.1, one can realize that the change in capillary pressure, due to small changes in void area, is negligible (maximum percentage of change is 1.9 %). By increasing tension, the ratio of P_D/P_C (dynamic pressure to capillary pressure) will rise up to 2.4 % at the same impact velocities.

During impact on fabrics, the droplet has the largest kinetic energy at its very impact point and gradually, the vertical movement of droplet will transform to a horizontal movement on the droplet [31]. Thus, droplet penetration occurs during impact in the cap section of broadening droplet (see Fig. 1b). The diameter of this cap is almost the same as the initial diameter of droplet and its vertical velocity can impart droplet liquid through voids [31]. In another words, droplet spreads without a large portion of the vertical velocity transferred into the horizontal one. Thus, available energy for spreading will be removed due to penetrated liquid.

To find the volume of removed liquid from droplet, total volume of voids of fabrics under the spreading cap of droplet (see Fig. 1b) should be calculated. In [4,32] drop impact on porous surfaces was studied and it was observed that volume of liquid that penetrates into voids is almost equal to the volume of the pores and empty spaces below the impact point on porous surfaces. No leakage from below the surface was reported in [4,32]; thus, the same can be deducted in our study. So, to calculate E_P, it is assumed that when the droplet impacts on the fabric, the volume of droplet is equal to the volume of fabric voids (in a circular area with a diameter of 3mm corresponding to the diameter before impact for penetration). The reason for considering this area is that maximum pressure is at the cap of droplet when the droplet impact on a surface [45]. Thus, penetrated droplet mass into voids remove energy from the liquid from spreading droplet; therefore, it can be assumed:

$$E_p = r_v . E_{k1} \quad (5.1)$$

In Equation 5.1, r_v is the fraction of droplet mass that penetrate into voids. To calculate r_v, total volume of voids in a circle with diameter of 3mm is measured for each fabric and then

divided by total volume of droplet. Table 5.2 below shows r_V for different fabrics at tension of 0.23 N for other amounts of tension, r_V is the same due to low changes in void size.

Table 5.2: Penetration ratio for droplet on different fabrics based on their void size

Fabrics	**r_v**
Satin weave	0
Warp weave	0.01
Weft weave	0.01
Plain weave	0.03
Mesh weave	0.05

According to Table 5.2, the percentage of energy dissipation by penetration will be 1 to 5 percent of total initial energy of droplet. For instance, on mesh weave, 5 percent of total initial energy will be removed through penetrated liquid. In order to perceive the significance of penetration, we have to calculate other energy dissipating parameters in Equation 2.1 and compare them in our final model, which is done in the following. It is noteworthy that detachment of satellite droplets below the fabric was not seen and droplets fill the voids completely. A question arises as to how it is claimed that droplet fill the voids completely and not partially. It is shown in [12] that when a droplet impact on a hydrophobic mesh (same as our fabrics), droplet will fill the voids completely (the velocities and void sizes are the same as our experiments).

5.2 Elastic Energy Results

5.2.1 Physical Interpretation

Impact of a droplet on a flexible surface, causes the surface to be deformed. Mangili et al. [33] considered the soft surface as series of springs that takes droplet energy during impact and they found that less energy remained for spreading and recoiling phase of the droplet. Deformation will dissipate some part of initial droplet energy, and there will be less energy for the spreading phase [34]. Thus, flexibility of surface may cause a decrease in maximum spreading of droplet.

5.2.2 Calculation

To calculate elastic energy which is stored in fabrics, we have to find the deflection of fabrics at the impact point. Table 5.3 shows the deflection of fabrics at 1.5 m/s for different fabric tensions. (for other velocities, see Appendix 1)

Table 5.3: Fabric deflection at drop impact velocity of 1.45 m/s for various tensions (deflection error is 0.02 mm)

Tension / Weaving	0.23 N	1.07 N	1.6 N
Satin weave	0.28 mm	0.23 mm (-18 %)	0.21 mm (-25 %)
Warp knit	0.49 mm	0.40 mm (-19 %)	0.36 mm (-27 %)
Weft knit	0.53 mm	0.44 mm (-17 %)	0.41 mm (-23 %)
Plain weave	0.89 mm	0.78 mm (-13 %)	0.72 mm (-20 %)
Mesh weave	1.05 mm	0.95mm (-12 %)	0.91 mm (-19 %)

It is noteworthy that elasticity of fabrics is different due to weave type. Having measured the deflections (dx), stored elastic energy on fabrics will be calculated by the Equation 5.2. This equation is not specified to deformation of a beam, disk, etc.; it is concerned with the work done during the deformation in this case a fabric. By multiplying the work with time (dt), the used energy will be obtained, as per force (F) applied by the mass of droplet (m) to cause a deflection (dx), as such:

$$E_e = \int\int F.dt.dx = \int\int m.\left(\frac{dv}{dt}\right).dt.dx = \int\int m.dv.dx \qquad (5.2)$$

To solve Equation 5.2, we have to define a function that relates the rate of deflection (v) and deflection. Thus, deflection of fabric should be measured; Figure 5.1 shows deflection as a function of time for mesh woven fabric at 1.45 m/s and tension of 0.23 N. (for other fabrics, see Appendix B). After 400 µs fabric will bounce back.

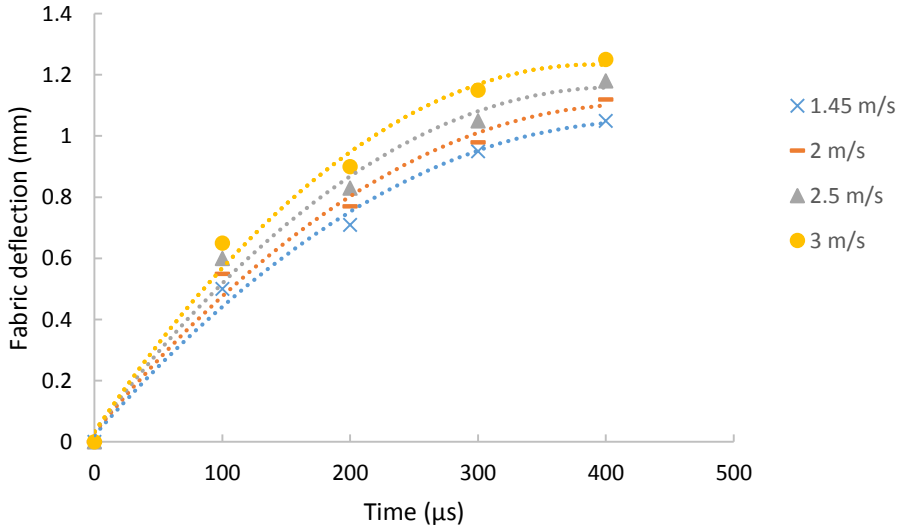

Figure 5.1: Deflection of mesh weave fabric at impact velocity of 1.45 m/s to 3 m/s at tension of 0.23 N from impact time to 400 µs.

It is known that velocity is dx /dt. Thus, by finding the tangent of the curves in Figure 5.1, one can find rate of deformations at each time. Figure 5.2 shows velocity as a function of deflection. (for other fabrics, see Appendix C)

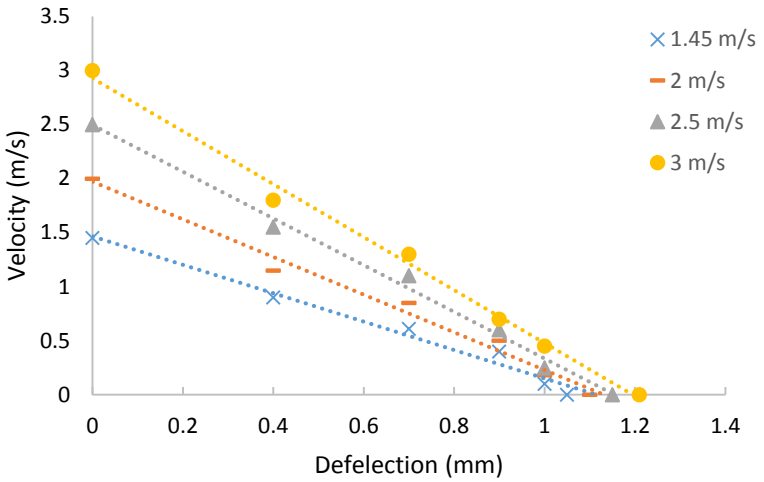

Figure 5.2: Deflection of mesh weave fabric as a function of velocity at impact velocities of 1.45 m/s to 3m/s, and tension of 0.23 N

As it is shown in Figure 5.2, trend lines show that deflection changes linearly by velocity. Thus, Equation 5.3 can be simplified as:

$$E_e = \int \int F.dt.dx = m.\Delta v.\Delta x \qquad (5.3)$$

A question arises as to why a one-dimensional formulation has been used while the deflection is a three dimensional phenomenon. The reason is that droplet movement is vertical and the main deflection of fabric will also be vertical. But, due to a very low amount of horizontal movement of fabric in comparison to its vertical movement, it is reasonable to neglect its horizontal movement. As a result, using a one-dimensional

equation is warranted. Equation 5.3 gives the deflection energy in each case, which is shown in Table 5.4 for 1.5 m/s of impact velocity (for other velocities refer to Appendix D and H).

Table 5.4: Droplet energy spent for fabric deflection at drop impact velocity of 1.45 m/s with different tensions (the error is 0.0008 μJ)

Fabric / Weaving	0.23 N	1.07 N	1.6 N
Satin weave	0.006 μJ	0.005 μJ	0.005 μJ
Warp knit	0.011 μJ	0.010 μJ	0.010 μJ
Weft knit	0.013 μJ	0.011 μJ	0.010 μJ
Plain weave	0.018 μJ	0.015 μJ	0.014 μJ
Mesh weave	0.021 μJ	0.017 μJ	0.015μJ

According to Table 5.4, E_d is much lower than initial kinetic, and surface energy of droplet due to low amount of fabric deflections. As it was expected, by increasing tension, E_d has been decreased due to lower deflection of fabrics at higher tensions.

5.3 Viscous Dissipation Energy Results

5.3.1 Physical Interpretation

In a viscous fluid flow, viscosity takes energy from the motion of the fluid (kinetic energy) and transforms it into internal energy. When a droplet spreads on a fabric, there is slip velocity at the wall. The droplet passes from top of the pores and voids that may be filled with penetrated liquid or air. Thus, on top of these voids, liquid is not in contact with any

solid surface and the velocity is not zero near the wall [32,35]. Furthermore, waviness of fabric perturbs the flow at the wall [34] which results in movement of liquid at the wall (non-zero velocity at the wall). Figure 5.3 shows the schematic view of velocity profile of spreading droplet.

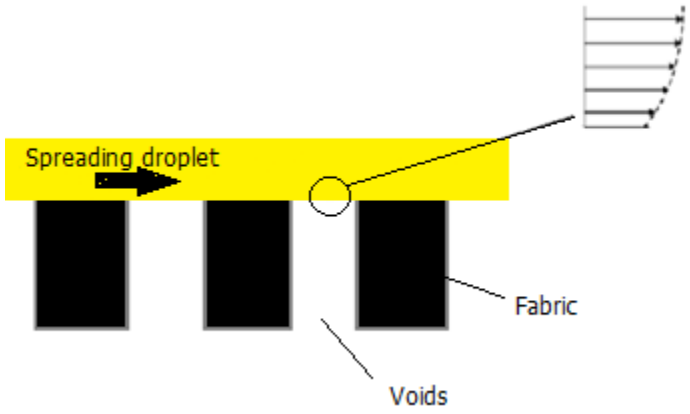

Figure 5.3: Schematic view of spreading droplet on fabrics

5.3.2 Calculation

To quantify the amount of dissipation through viscous forces, the amount of viscous dissipation in spreading phase needs to be calculated by Equation 5.4 [36]. Some previous works on drop impact on porous surfaces, have neglected viscous dissipation due to low viscosity of water [4]. But, Lembach et al. [32] observed that when the droplet moves on porous surfaces, the spreading velocity changes proportional to the inverse of diameter of spreading droplet. In another work, Joung and Buie [35] found that while drop moves on porous surfaces, the velocity at the lamella is a linear function of distance from impact point. Besides, Muschi et al. [37] found that when the droplet impact on SLIPS surfaces, viscous dissipation inside the spreading droplet is much larger than viscous dissipation

inside the liquids in the pores. They show that the viscous dissipation in the voids during the spreading stage is negligible compared to the viscous dissipation in the water drop and cannot affect maximum diameter of droplet. It is found in [37] that boundary layer in the droplet is much larger (ten times in their case) than the boundary layers inside pores, and droplet spreading on air or liquid-filled pores cannot affect maximum spreading of droplet. Thus, it can be assumed that in our work that boundary layer inside pores cannot affect viscous dissipation. In another work, Lee et al. [38] found that when the pores are filled by air, viscous forces are lower at contact line compare to the liquid-filled pores; but, they claimed that this amount of viscous dissipation is negligible compare to the one inside droplet. Thus, it can be understood that viscous dissipation of penetrated liquid cannot affect droplet behavior or maximum spreading droplet.

In both [32,35], it is hypothesized that spreading velocity will change almost linearly from the wall to top of the droplet in the droplet at the lamella and as a result, slip velocity will also change linearly. In order to measure slipping velocity at the wall, they [32,35] measured ratio of thickness changing of spreading droplet and found the average velocity of droplet at each time. By calculating average velocity and knowing the spreading velocity (recorded from videos), they estimated the slip velocity at the wall.

Due to the fact that fabrics are porous, slip velocity will be present on the surface of fabrics. The porosity of the fabric results in drag reduction supported by a shear air-water interface (rather than solid-water interface) over which water slips [39]. So, Equation 5.4 is used for cases with slip velocity, because despite most of the models that consider no slip condition near the wall, slip velocity has been considered near surface. Equation 5.4 is written

between the moment of impact and the moment of maximum spreading diameter (R_{max}) [32].

$$E_v = \int \tau . V . dA = [3(\Psi/We).R_{max}^{\ 2}.(dr/dt)^2.A_s/A_p]. \Delta t \quad (5.4)$$

$$\Psi = \pi/(Oh)^{0.5}$$

In Equation 5.4, Δr is the difference between the initial diameter, and the maximum spreading diameter of droplet; Δt is the time from impact to the maximum spreading. In Equation 5.4, the parameter dA was used for smooth surfaces and integration was done on a plain surface [32]. However, in this work recognizing the surface waviness, we modified the original form of the Eq. 5, by multiplying the term dA by A_s/A_p (surface area divided by projected area) to meet the surface condition exactly.

Since the viscous dissipation calculations [32] is done from impact time, the reference time in tables and plots is impact time.

Table 5.5 shows the viscous dissipations for drop spreading on different fabrics, from the impact time to maximum spreading of droplet at 1.45 m/s of impact velocity (for other velocities refer to Appendix E).

Table 5.5: Viscous dissipation energy at 1.45 m/s of drop impact velocity at different tensions (error is 0.016 μJ)

Fabric / Weaving	0.23 N	1.07 N	1.6 N
Satin weave	0.19 μJ	0.19 μJ	0.18 μJ
Warp knit	0.22 μJ	0.21 μJ	0.21 μJ
Weft knit	0.23 μJ	0.23 μJ	0.23 μJ
Plain weave	0.25 μJ	0.25 μJ	0.25 μJ
Mesh weave	0.26 μJ	0.26 μJ	0.26 μJ

According to Table 5.5, and by comparing these values with the initial total energy of droplet, viscous dissipation is in the order of 0.28 μJ. Additionally, as mentioned before, by increasing tension no considerable changes were observed in droplet behavior and maximum spreading of droplet. Thus, no difference was seen in viscous dissipations at different tensions.

5.3.3 Waviness Physical Interpretation

Surface waviness is the periodic component of surface texture. It was observed that during movement of droplet on surfaces with waviness (the used word in their study), maximum droplet diameter will be lower, compared to smooth surfaces [16]. It was found that when the droplet moves on surfaces with undulation, the droplet surface will be affected considerably. Kalliadasis and Bieralz [40] realized that during movement of liquid on surface topography, the lower side of liquid which is in contact with the surface, will take the shape of the topography of surface (they did not mention the word waviness; but, they measured surface undulation at large cut-off values (order of 1mm) which is only used for measuring waviness and not roughness). Unfortunately, they did not provide any physical explanation for this behavior. As a result, one can expect that droplet surface area and

surface energy will be increased when the droplet moves on fabrics compared to smooth surfaces. This is due to the fact that surface area (A_S) is larger than projected area (A_P) on textiles. The closer A_S gets to A_P, the smoother surface becomes.

5.3.4 Waviness Calculation

To calculate surface energy considering surface waviness Equation 5.5 is used for a spreading droplet.

$$E_{S2}=\Upsilon_{lv}.\pi.r^2 + \Upsilon_{sl}.\pi.r^2.\frac{As}{Ap} \quad (5.5)$$

The first term in Equation 5.5 is related to surface energy of droplet (upper surface of spreading droplet which is in contact with ambient air). The second term is for surface energy of lower side of droplet which is in contact with fabrics. The reason that this term is multiplied by $\frac{As}{Ap}$ is that the surface of fabric is not flat. Thus, the area which is seen from the top view is not the actual surface area. For instance, on satin woven fabric, top view area is 11.13 μm^2 (which is projected area and the size of fabric), the actual area is 27.78 μm^2 considering its waviness. Thus, the bottom area of a spreading droplet that has the radius of R from top view is calculated:

$11.13/ \pi R^2 = 27.78/(\text{bottom area})$

therefore,

$\text{Bottom area} = (27.78/11.13).\pi R^2 = \frac{As}{Ap} . \pi R^2$

Table 5.6 shows the surface energies of droplet on different fabrics at 1.5 m/s at maximum spreading diameter (see Appendix F and H).

Table 5.6: Surface energies of fabrics at maximum spreading of droplet at drop impact velocity of 1.45m/s (error is 0.7 µJ)

Tension / Weaving	0.23 N	1.07 N	1.6 N
Satin weave	15.96 µJ	16.10 µJ	16.18 µJ
Warp knit	15.95 µJ	15.97 µJ	15.97 µJ
Weft knit	15.94 µJ	15.96 µJ	15.96 µJ
Plain weave	15.85 µJ	15.97 µJ	16.03 µJ
Mesh weave	15.74 µJ	15.84 µJ	15.89 µJ

Referring to Table 5.6, the order of magnitude of surface energy is comparable to the initial total energy of droplet, which indicates that waviness have the most effect in droplet energy conversion while spreading. This is a distinguishing discovery in this work compared to the literature for drop impact for solid surfaces (smooth or rough) that had no waviness. In other words, most of the initial total energy of droplet has been transformed to surface energy of spreading droplet that is affected by waviness of fabrics.

5.4 Final Formulation of Model

Based on the previous sections of this chapter, it would be possible to predict the maximum radius of droplet on fabrics with different topographies. Thus, Equation 2.1 for fabrics can be formulated as:

$$\gamma_{lv}\pi.r_1^2 + 1/2mU^2 = r_v.\, E_{k1} + \int\int F.dt.dx + [3\,(\Psi/We).R^2.(dR/dt)^2.A_s/A_p].\,\Delta t + \gamma_{lv}.\pi.R^2 + \gamma_{sv}.\pi.R^2.A_S/A_p \quad (5.6)$$

5.5 Energy Analysis

Figures 5.4 to 5.7 show experimental value of energy balance for each fabric of various drop impact velocities. (see Appendix H)

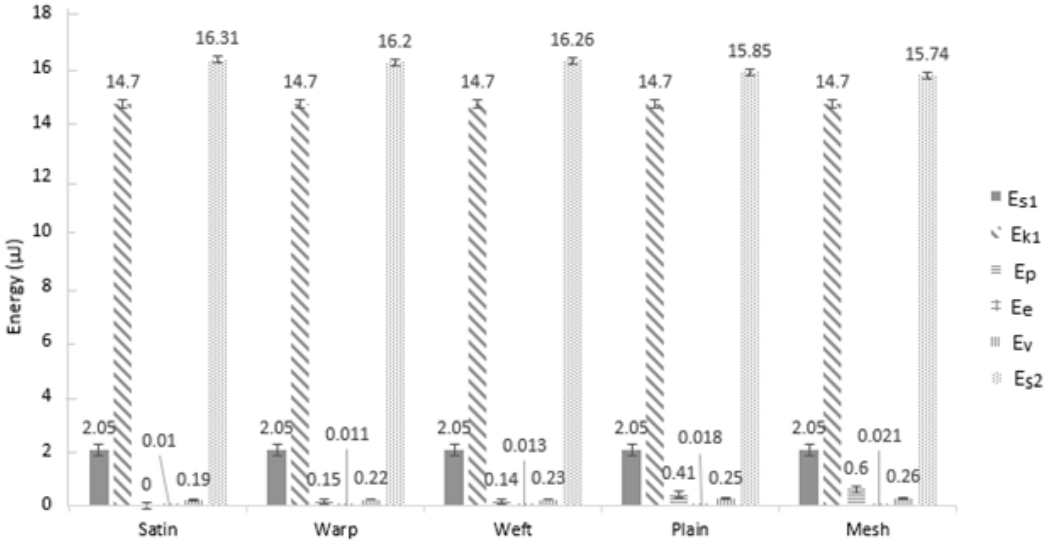

Figure 5.4: Component of energy equation (Eq. 5.6) for each of the fabrics studied at impact velocity of 1.45 m/s

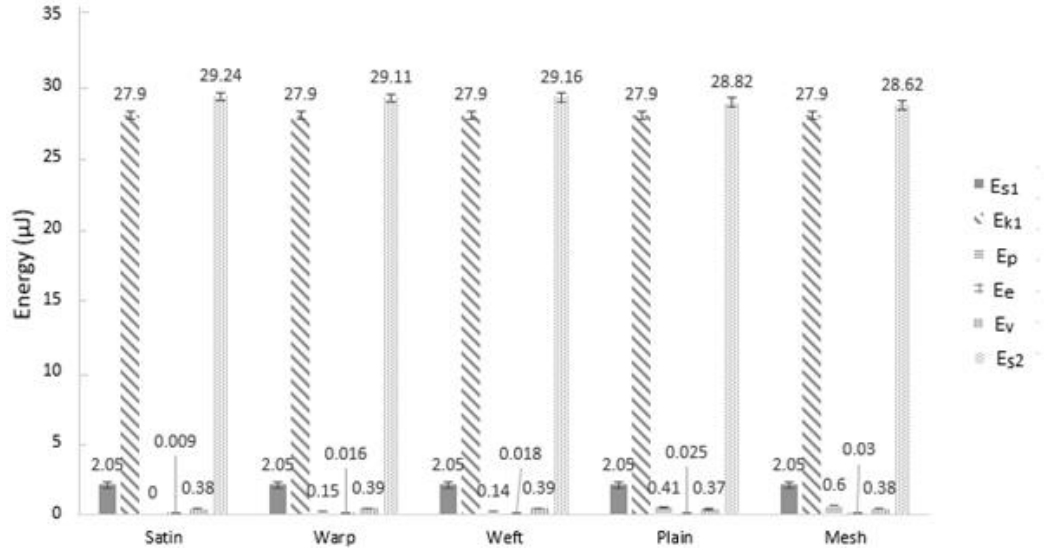

Figure 5.5: Component of energy equation (Eq. 5.6) for each of the fabrics studied at impact velocity of 2 m/s

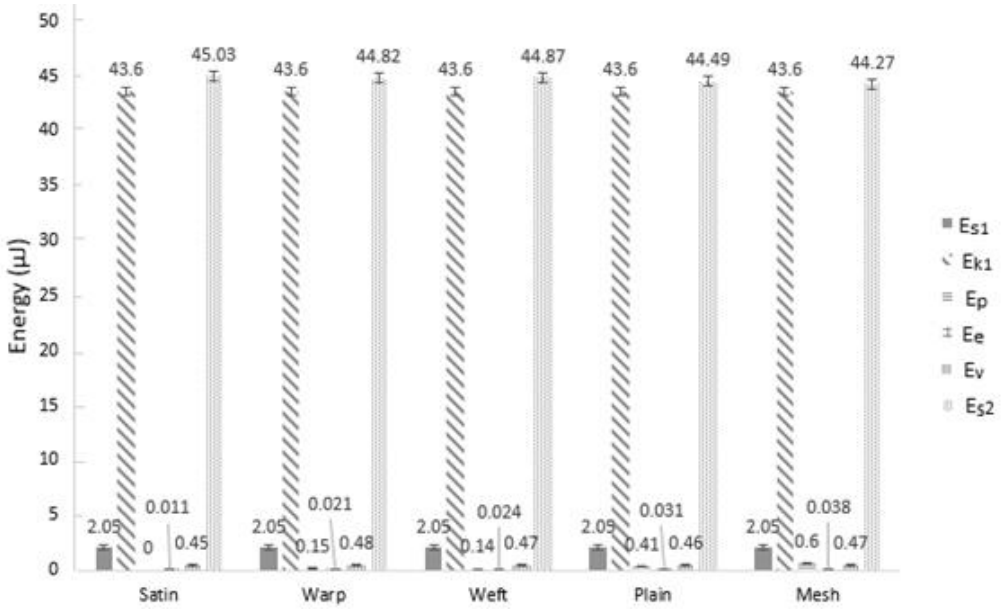

Figure 5.6: Component of energy equation (Eq. 5.6) for each of the fabrics studied at impact velocity of 2.5 m/s

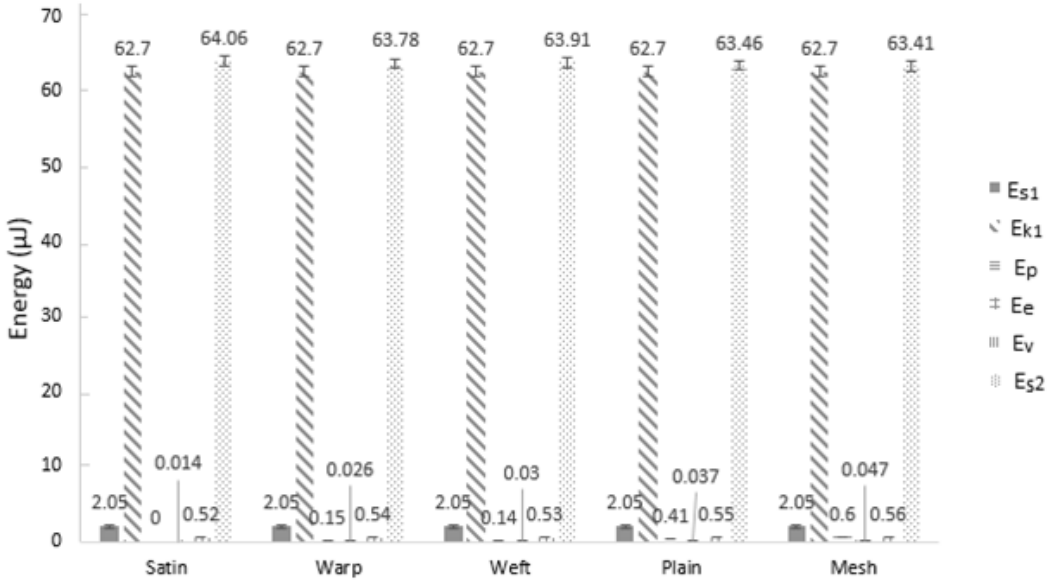

Figure 5.7: Component of energy equation (Eq. 5.6) for each of the fabrics studied at impact velocity of 3 m/s

As it is shown in Figures 5.4 to 5.7, the most part of initial total energy of droplet is transformed to surface energy as droplet spreads. Viscous dissipation and E_P are the next important factors in the energy balance analysis. Therefore, considering parameters which are larger compare to other parameters, the only important parameter would be the surface energy. Thus, we can rewrite Equation 5.6 in the simplified form of:

$$E_{S1} + E_{k1} \approx \Upsilon_{lv}\pi R^2 + \Upsilon_{sl}\pi R^2 A_s/A_p \quad (5.7)$$

Apart from calculations, it could be understood from observations in previous chapter that, deflection energy would be negligible due to similar behavior of droplet at different tensions. Also, increasing tension will not change void size and E_p due to similar behavior of droplet at different tensions that showed E_p would be negligible in the introduced model on our fabrics. Besides, observing increase in diameter of droplet at higher velocity would be due to the fact that most of the initial energy of droplet may be transformed to surface energy and E_{S2} would be the governing factor in determining droplet behavior.

To make Equation 5.7 independent of droplet diameter, it is reshaped in non-dimensional form as in Equation 5.8:

$$4 + We/3 = D_N{}^2(1+(A_s/A_p)\,\Upsilon_{sl}/\Upsilon_{lv}) \quad (5.8)$$

In Equation 5.8, D_N is the non-dimensional diameter of droplet which is defined as droplet diameter at maximum spreading divided by initial diameter of droplet.

5.6 Validity of Equation 5.8

Based on Equation 5.8, we can introduce a model for prediction of maximum diameter of droplet on fabrics and compare to experimental results with this model. Figures 5.8 to 5.11 show the comparison of prediction of model and symbols show the results from experiments at impact velocities of 1.45 m/s, 2 m/s, 2.5 m/s and 3 m/s and tension of 0.23N on all fabrics and on coated glass (see Appendix H).

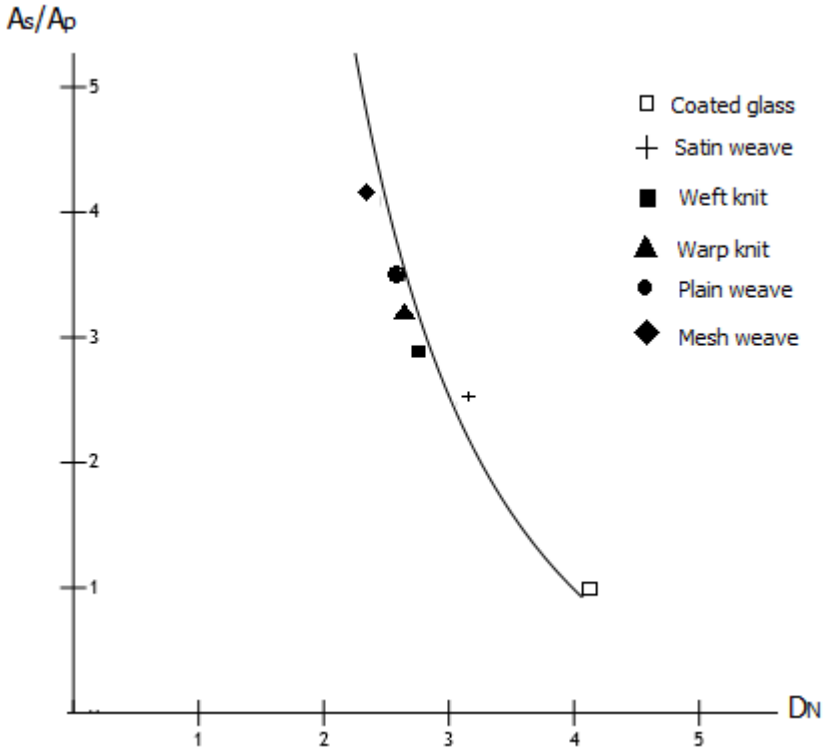

Figure 5.8: The plot from Equation 5.8 and experimental results at impact velocity of 1.45 m/s (error is 0.2 mm)

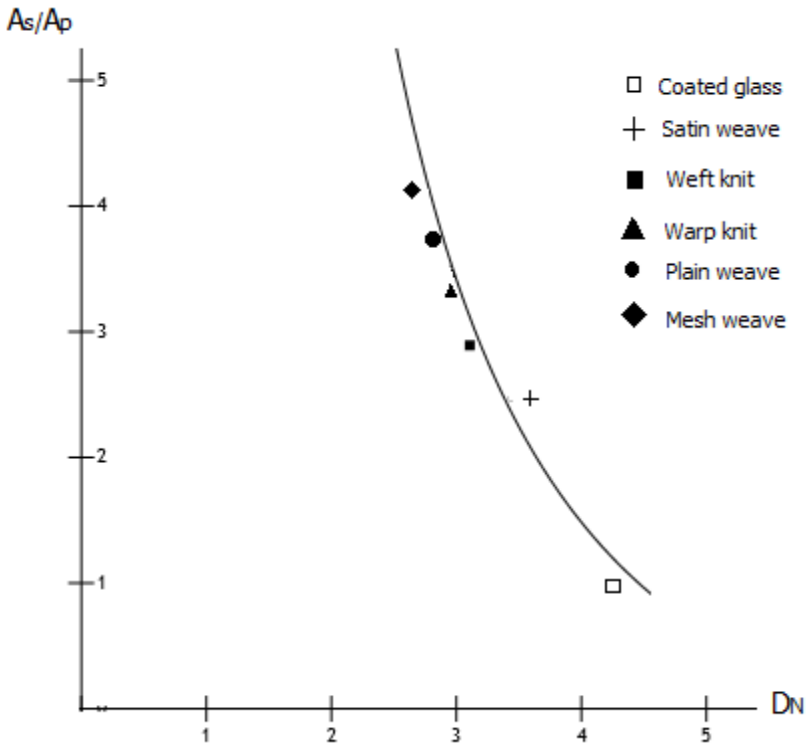

Figure 5.9: The plot from Equation 5.8 and experimental results at impact velocity of 2 m/s (error is 0.2 mm)

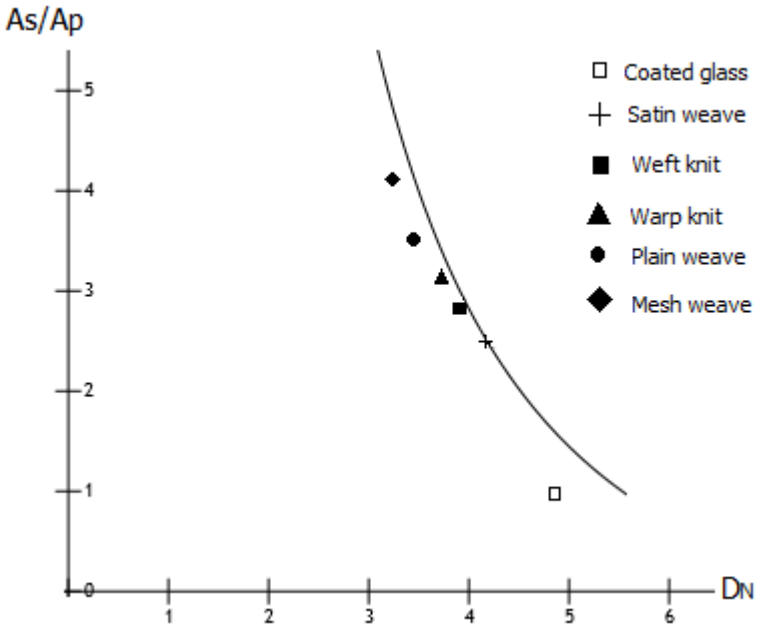

Figure 5.10: The plot from Equation 5.8 and experimental results at impact velocity of 2.5 m/s (error is 0.2 mm)

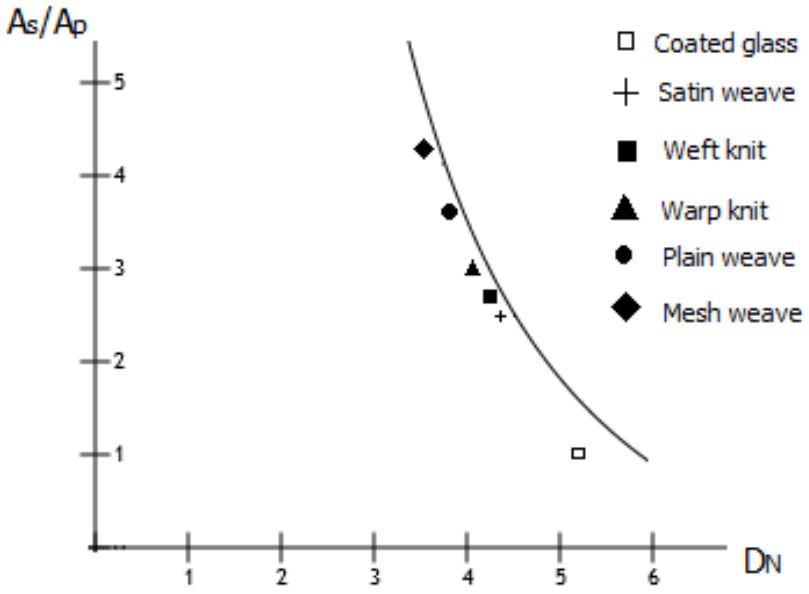

Figure 5.11: The plot from Equation 5.8 and experimental results at impact velocity of 3 m/s (error is 0.2 mm)

According to Figures 5.8 to 5.11, the introduced model is in good agreement with the experimental results that validate our model. Mathematically, the asymptote line in Figures 5.8 to 5.11 is at D_N=1 mm at higher A_s/A_p. This means by increasing A_s/A_p, maximum spreading diameter of droplet will be decreased due to larger area at liquid-solid interface. But, if undulation of the surface is considered as a sinusoidal plot, wavelength and amplitude of fabrics cannot be more than 3 mm (diameter of droplet); because for larger amounts droplet will be trapped between two peaks of fabrics and cannot spread then (see Figure 5.12)

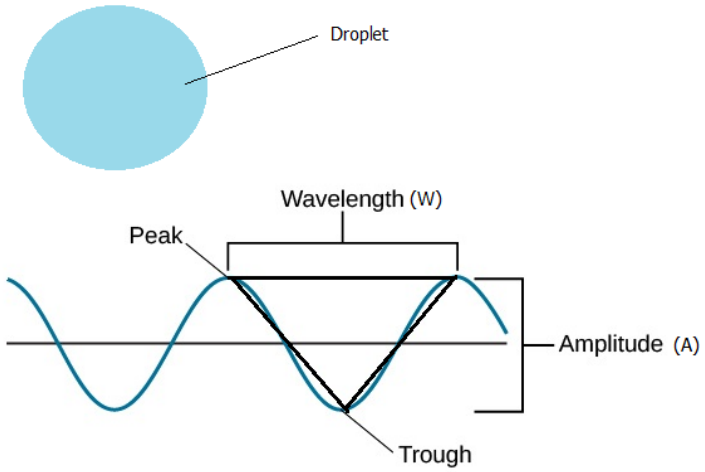

Figure 5.12: Schematic of fabric wavelength and Amplitude

In order to calculate A_S/A_p as a function of waviness and amplitude, the area between two peaks has been considered as a sinusoidal pattern; The result of dividing length of plot between two peaks to wavelength A_S/A_p will be derived. Thus

$$A_S/A_p = 2((W/2)^2+A^2)^{0.5}/W = (1+(2A/W)^2)^{0.5} \quad (5.9)$$

The lowest diameter of a thread of fabrics (in industry) is 0.2 mm [41] and in each wavelength consist of at least two threads plus spacing between them. Thus,

$0.4mm < W < 3mm \ \& \ 0 < A < 3mm$

Based on Equation 5.8, largest amount of A_S/A_p is at lowest wavelength and largest amplitude; therefore,

$1 < A_S/A_p < 15$

Thus, for A_S/A_p larger than 15, results of the model will be physically meaningless. As it is shown in Figures 5.8 to 5.11, maximum diameter of droplet is the largest on coated glass

surface (A_s/A_p=1). This is due to the fact that on coated glass surfaces, there is no undulation and droplet moves easier on smooth surfaces. It is noteworthy that the introduced model will be physically meaningless at A_s/A_p<1; because, surface area cannot be smaller than projected area. Besides, there is no asymptote line at A_S/A_P=1; because, if it was, maximum diameter of droplet would be infinite which is physically impossible. Predicted results of our model for different velocities are shown in Figure 5.13.

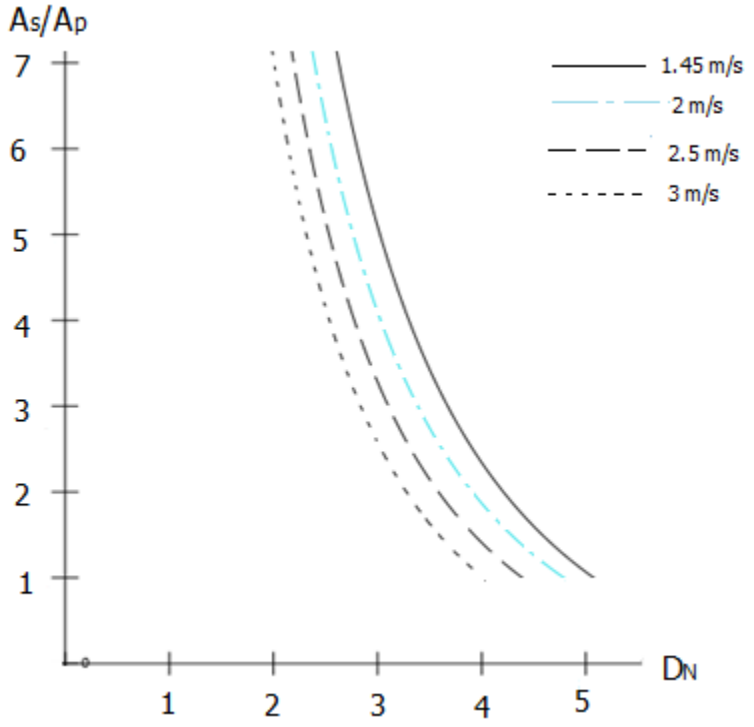

Figure 5.13: Non-dimensional maximum diameter of droplet at different velocities (error is 0.2 mm)

As it is shown in Figure 5.13, by increasing impact velocity, the maximum spreading of diameter will be increased. With this plot one can predict maximum spreading of droplet at different velocities as well. Furthermore, the plot in Figure 5.13 will be close to D_N=1 at

larger A_s/A_p which is expected, due to the fact that the maximum spreading of droplet cannot be smaller than its initial diameter and as a result D_N cannot be smaller than 1.

5.7 Validity of model for coated glass surface and comparison with other models

To investigate whether the model works properly for smooth surfaces, it has been compared with the model by Ukiwe et al. [42] and Roisman et al [43]. Their model was selected for comparison, because they introduced the model by balancing energy between initial total energy and surface energy and viscous dissipation; and for validating their model they studied drop impact on polyester (PS) surface (same as surface used in our work). They compared the maximum diameter of droplet from their results with their model. Their results were in good agreement with their model and showed a mere 5% difference in maximum diameter of droplet between their model and experimental results.

The final model in their work was introduced as follows:

$$(We+12)\ D_N = 8 + D_N^3.[3(1-\cos(\theta))+4.We/(Re^{0.5})] \quad ; D_N \text{ is non-dimensional diameter} \tag{5.10}$$

Figure 5.14 shows the non-dimensional maximum diameter for drop impact on surface PS coated glass based on their model and model developed in this work (Equation 5.8).

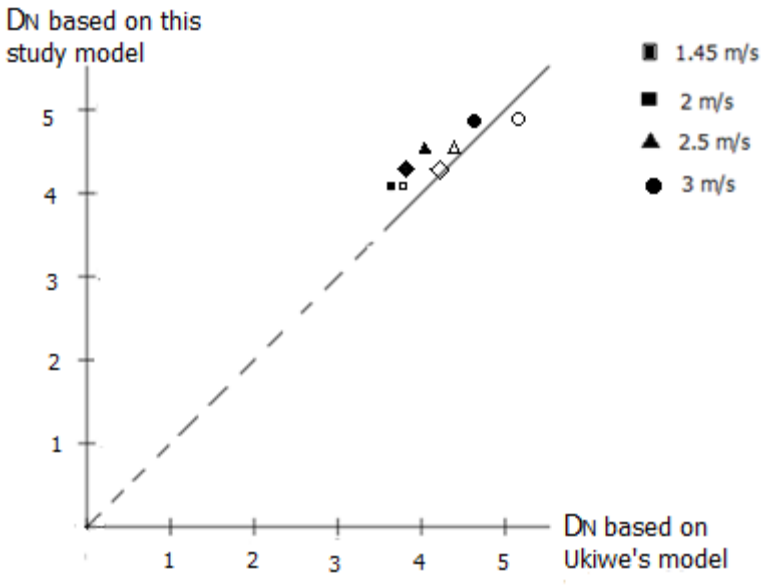

Figure 5.14: Non-dimensional maximum diameter of droplet on model developed in this work and that of Ukiwe et al [42] (solid symbols) and Roiman et al [43] (empty symbols).

The dotted line in Figure 5.14 has a slope of 45 degrees, and is used to compare the results from the model developed in this study to that of Ukiwe et al [42] and Roisman et al [43]. As it is shown in Figure 5.14, results match almost perfectly. The difference between these models is less than 8% (For the impact velocity of 2.5 m/s). This question comes in mind that why Roisman's model is different from Ukiwe's model. In Ukiwe's model, they incorporated viscous dissipation and surface tension effects in their simultaneous solution of fluid kinetics and drop spread termination is dictated exclusively by surface tension and viscous energy dissipation. While Roisman developed a model for the time dependent droplet spreading ratio, by solving the mass and the momentum equations of the rim appearing at the edge of the spreading droplet within which liquid is bounded. In Roisman's

model, they considered wettability, surface tension, viscous dissipation and inertia have been accounted for spreading ratio calculation.

5.8: Prediction of droplet behavior on fabrics with higher r_v

As mentioned previously, by increasing r_v, volume of voids will be increased. Consequently, the amount of removed energy by penetration will be increased (E_p). Thus, less energy will remain for spreading phase of droplet. Therefore, by taking r_v into account the final non-dimensional model will be:

$$4+(1-r_v).\ We/3= D_N^2.(1+(A_s/A_p).\ \Upsilon_{sl}/\ \Upsilon_{lv}) \quad (5.11)$$

In Figure 5.15, the results (D_N) based on Equation 5.11 at different amount of r_v values (0, 0.2 and 0.4) for impact velocity of 1.45 m/s (as an example) are compared.

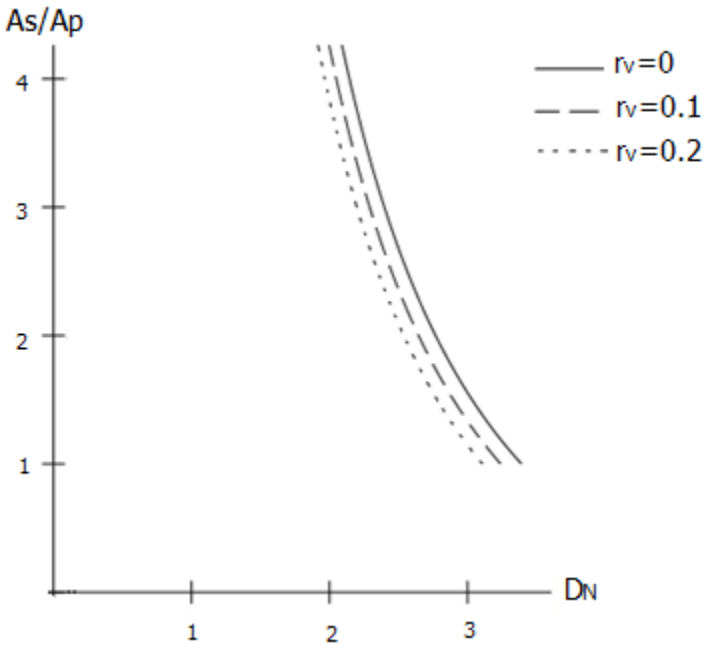

Figure 5.15: Non-dimensional maximum diameter of droplet at impact velocity of 1.45 m/s and different r_v

(r_v=0 is for smooth surfaces with no undulations and zero amplitude)

Increasing r_v means more mass transfer from system into voids and less energy for spreading phase. As it is shown in Figure 5.15, by increasing r_v, maximum diameter of droplet has been decreased at the same As/Ap. This is due to the fact that, on fabrics with higher r_v, amount of penetrated liquid through voids will be increased and less energy will remain for spreading phase of droplet. Therefore, maximum spreading of droplet will be decreased. (same trend is observed for all impact velocities). Furthermore, by comparing results of experiments in Figures 5.8 to 5.11 with the model in this work, it can be verified that our results are in good agreement with this model. As an example, maximum diameter of droplet on mesh woven fabric (r_v=0.05) is compared with the model in Figure 5.16.

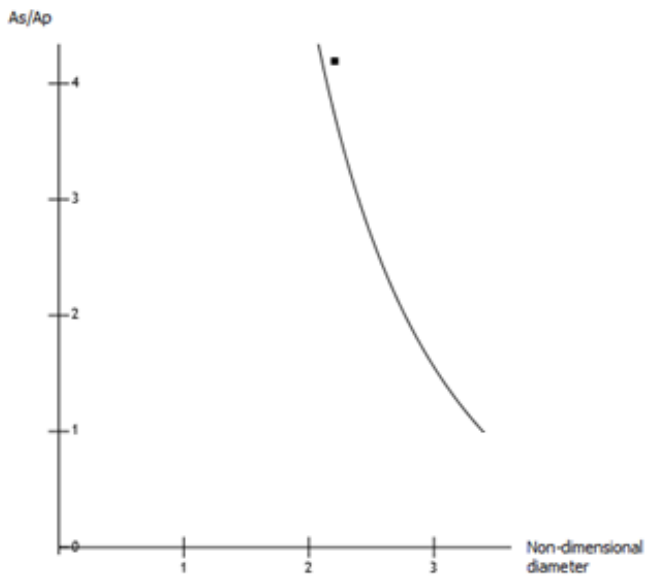

Figure 5.16: Non-dimensional maximum diameter of droplet at impact velocity of 1.45 m/s on mesh weave. The point shows experimental result at this impact velocity and on this fabric

5.9 Effect of Velocity

Based on literature, by increasing droplet impact velocity, kinetic energy of droplet will be increased; therefore, the maximum diameter of droplet will be increased [42]. Figures 5.17 to 5.21 show non-dimensional diameter as a function of droplet impact velocity and compared with experimental results.

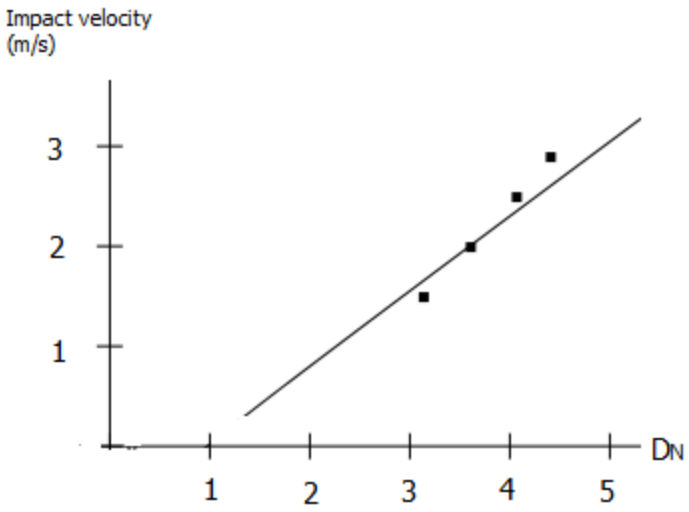

Figure 5.17: Maximum non-dimensional diameter at different impact velocities for Satin woven fabric. Points show experimental results (error is 0.2 mm)

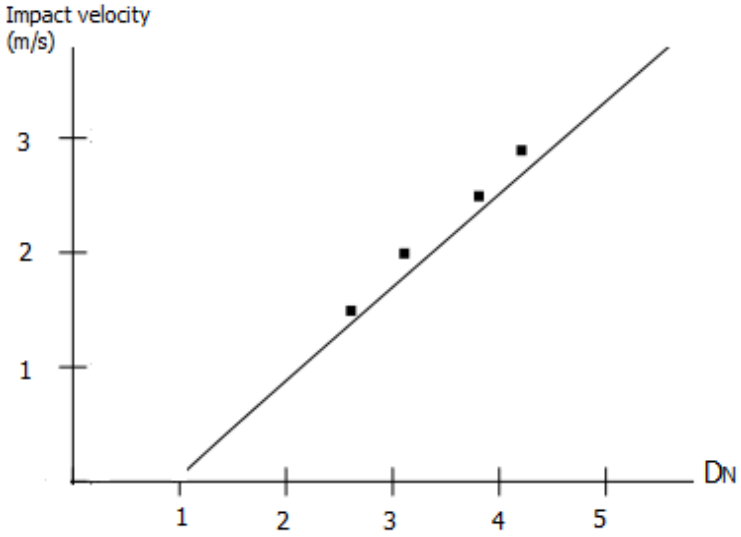

Figure 5.18: Maximum non-dimensional diameter at different impact velocities for warp knitted fabric. Points show experimental results (error is 0.2 mm)

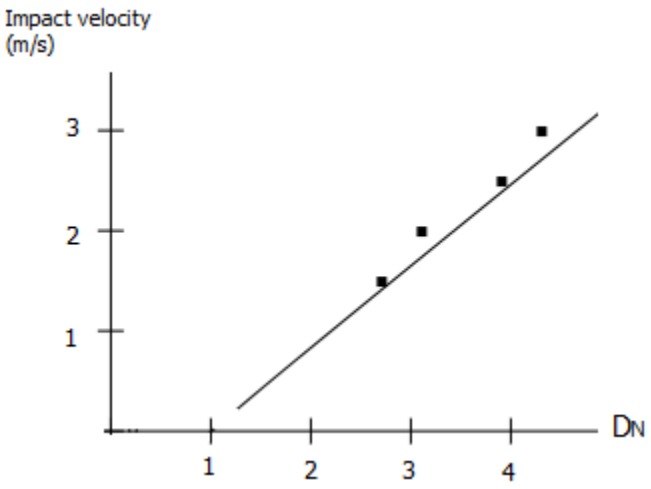

Figure 5.19: Maximum non-dimensional diameter at different impact velocities for weft knitted fabric. Points show experimental results (error is 0.2 mm)

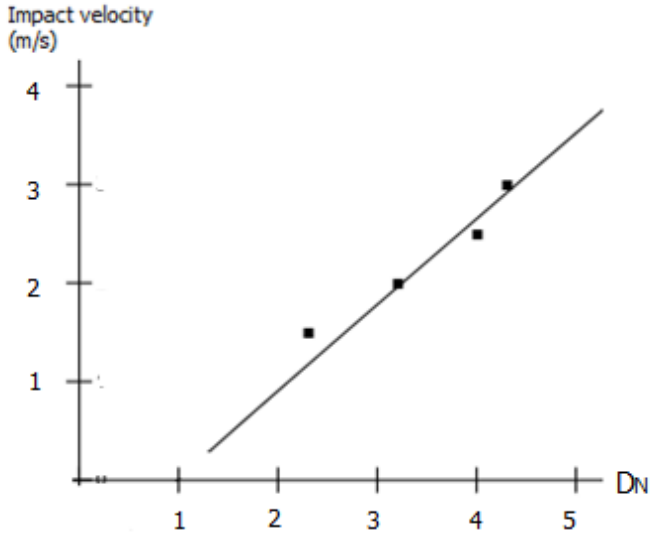

Figure 5.20: Maximum non-dimensional diameter at different impact velocities for Plain woven fabric. Points show experimental results (error is 0.2 mm)

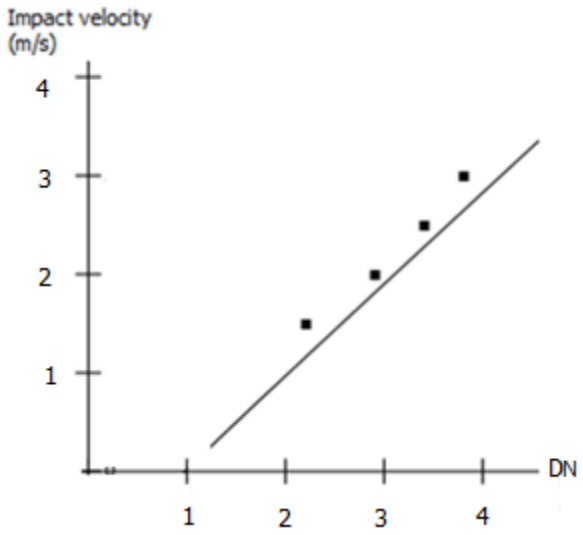

Figure 5.21: Maximum non-dimensional diameter at different impact velocities for mesh woven fabric. Points show experimental results (error is 0.2 mm)

According to Figures 5.17 to 5.21, the experimental results are in good agreement with the model. As it was expected, by increasing velocity, maximum spreading diameter of droplet has been increased. Additionally, based on this model diameter of droplet at different impact velocities can be calculated.

Based on the model in this work, diameter of droplet on fabrics with different waviness as a function of velocity is calculated. Figure 5.22 shows the results from our model.

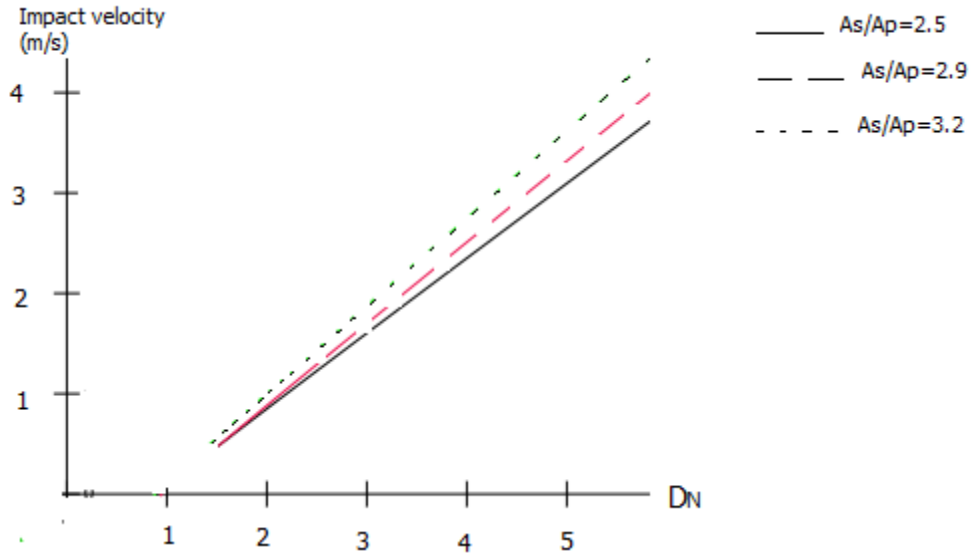

Figure 5.22: Maximum non-dimensional diameter as a function of impact velocity at different A_s/A_p (error is 0.2 mm)

As it is shown on Figure 5.22, by increasing waviness (A_s/A_p), maximum diameter of droplet will be decreased.

5.10 Time for reaching maximum diameter

Figure 5.23 shows the time for reaching maximum diameter on Satin woven fabric at different tensions (for other fabrics refer to Appendix G).

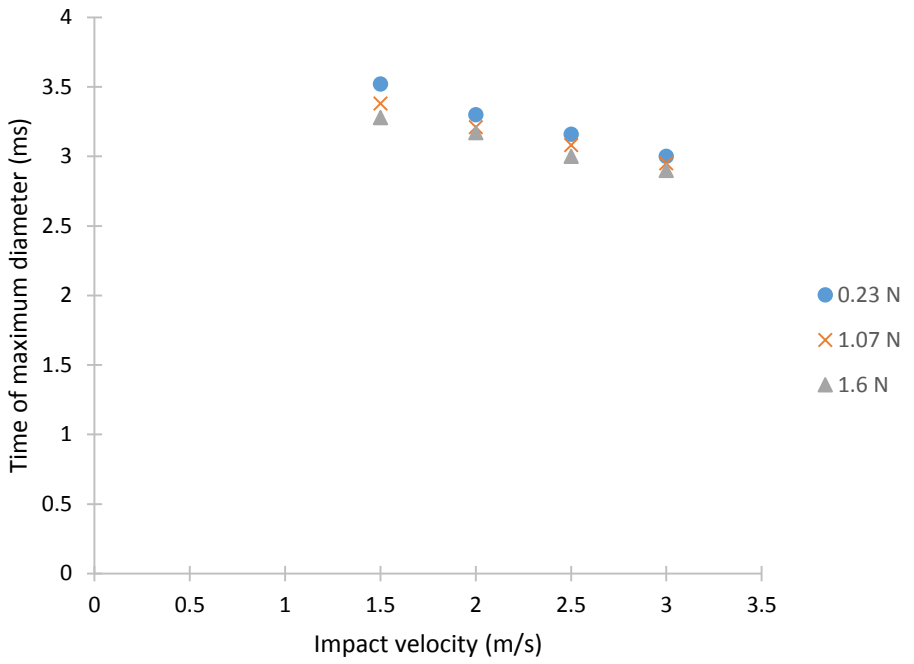

Figure 5.23: Time for reaching maximum diameter of droplet on satin weave at different droplet impact velocities

From Figure 5.23 it can be concluded that increasing drop impact velocity leads to a faster spreading of droplet which is in agreement with previous studies [40]. By increasing drop impact velocity, due to higher initial energy of droplet, it will reach faster to its maximum diameter.

Another point is related to effect of fabric tension on time for reaching the maximum diameter. Based on Equation 4:

$$E_e = m.dV.dx \qquad (5.12)$$

The order of energy for elastic energy is much smaller than the total energy. Thus this amount cannot change dynamics of droplet drastically. But, it should not be neglected. As it is seen in Figure 5.23, by increasing tension, time for reaching the maximum diameter

was decreased minimally (the changes are approximately 0.1 ms). The reason is related to the fact that by increasing tension, deflection of fabric will be decreased and more energy will remain for spreading phase that cause faster spreading of droplet (because E_e is small, the changes in time are also small).

Chapter VI: Conclusion and Future works

An experimental study on drop impact on fabrics was performed. Droplets with different velocities impact on fabrics with different weaving type. A model from energy point of view is introduced for prediction of droplet behavior on fabrics and validated by experimental results. It was found that when the droplet impact on fabrics, droplets liquid penetrates into voids and fill the voids; but, this amount of liquid penetration is not enough to affect droplet behavior in spreading phase due to low volume of voids compare to volume of droplet. Also, the effect of fabric deflection on dynamics of droplet was investigated. It was found that due to small deflection of fabrics at impact point, stored elastic energy is not large enough compare to droplet total energy and will not affect droplet behavior. It was found that the most part of initial total energy of droplet is transformed to surface energy at maximum spreading of droplet. The important point is that apart from impact velocity, maximum spreading of droplet depends highly on waviness of surface of fabrics. It is understood that, on surfaces with higher waviness, droplet maximum spreading diameter will be decreased due to increase in solid-liquid interface. Although fabric tension does not affect droplet behavior at spreading phase, it causes faster spreading of droplet at higher fabric tensions.

Based on insight gained through this experimental study on droplet impact on fabrics, some future works can be proposed. In drop impact on fabrics, the material of fabric is a key factor in droplet behavior and other materials with different hydrophobicity can be examined. Being able to change wavelength and amplitude of fabric undulation can help in defining a border that the introduced model would be applicable in according to droplet diameter.

References

[1] Tao, X. (Ed.). (2001). Smart fibres, fabrics and clothing: fundamentals and applications. Elsevier.

[2] Kubiak, K. J., Wilson, M. C. T., Mathia, T. G., & Carval, P. (2011). Wettability versus roughness of engineering surfaces. Wear, 271(3-4), 523-528.

[3] Hartley, G. S., & Brunskill, R. T. (1958). Reflection of water drops from surfaces. Surface Phenomena in Chemistry and Biology, 214.

[4] Rioboo, R., Voué, M., Vaillant, A., & De Coninck, J. (2008). Drop impact on porous superhydrophobic polymer surfaces. Langmuir, 24(24), 14074-14077.

[5] Antonini, C., Amirfazli, A., & Marengo, M. (2012). Drop impact and wettability: From hydrophilic to superhydrophobic surfaces. Physics of Fluids, 24(10), 102104.

[6] Range, K., & Feuillebois, F. (1998). Influence of surface roughness on liquid drop impact. Journal of Colloid and Interface Science, 203(1), 16-30.

[7] Wenzel, R. N. (1949). Surface roughness and contact angle. The Journal of Physical Chemistry, 53(9), 1466-1467.

[8] Mundo, C. H. R., Sommerfeld, M., & Tropea, C. (1995). Droplet-wall collisions: experimental studies of the deformation and breakup process. International Journal of Multiphase Flow, 21(2), 151-173.

[9] Josserand, C., & Thoroddsen, S. T. (2016). Drop impact on a solid surface. Annual Review of Fluid Mechanics, 48, 365-391.

[10] Latka, A., Boelens, A. M., Nagel, S. R., & de Pablo, J. J. (2018). Drop splashing is independent of substrate wetting. Physics of Fluids, 30(2), 022105.

[11] Lorenceau, É., & Quéré, D. (2003). Drops impacting a sieve. Journal of Colloid and Interface Science, 263(1), 244-249.

[12] Ryu, S., Sen, P., Nam, Y., & Lee, C. (2017). Water penetration through a superhydrophobic mesh during a drop impact. Physical Review Letters, 118(1), 014501.

[13] Soto, D., Girard, H. L., Le Helloco, A., Binder, T., Quéré, D., & Varanasi, K. K. (2018). Droplet fragmentation using a mesh. Physical Review Fluids, 3(8), 083602.

[14] Boscariol, C., Sarker, D., Chandra, S., & Marengo, M. (2018). Drop impact onto suspended and surface-attached metallic meshes: liquid penetration and spreading.

[15] Pepper, R. E., Courbin, L., & Stone, H. A. (2008). Splashing on elastic membranes: The importance of early-time dynamics. Physics of Fluids, 20(8), 082103.

[16] Calvimontes, A., Badrul Hasan, M. M., & Dutschk, V. (2010). Effects of Topographic Structure on Wettability of Woven Fabrics. Woven Fabric Engineering. 1st ed. Sciyo, 71-92.

[17] Romdhani, Z., Baffoun, A., Hamdaoui, M., & Roudesli, S. (2014). Drop impact on textile material: effect of fabric properties. Autex Research Journal, 14(3), 145-151.

[18] Romdhani, Z., Baffoun, A., Hamdaoui, M., & Roudesli, S. (2017). Experimental study and mathematical model to follow the spreading diameter on coated woven cotton fabric. Fibers and Polymers, 18(12), 2454-2461.

[19] Dussan, E. B. (1979). On the spreading of liquids on solid surfaces: static and dynamic contact lines. Annual Review of Fluid Mechanics, 11(1), 371-400.

[20] Šikalo, Š., Wilhelm, H. D., Roisman, I. V., Jakirlić, S., & Tropea, C. (2005). Dynamic contact angle of spreading droplets: Experiments and simulations. Physics of Fluids, 17(6), 062103.

[21] Blake, T. D., Bracke, M., & Shikhmurzaev, Y. D. (1999). Experimental evidence of nonlocal hydrodynamic influence on the dynamic contact angle. Physics of Fluids, 11(8), 1995-2007.

[22] Shikhmurzaev, Y. D. (1997). Moving contact lines in liquid/liquid/solid systems. Journal of Fluid Mechanics, 334, 211-249.

[23] Fukai, J., Shiiba, Y., Yamamoto, T., Miyatake, O., Poulikakos, D., Megaridis, C. M., & Zhao, Z. (1995). Wetting effects on the spreading of a liquid droplet colliding with a flat surface: experiment and modeling. Physics of Fluids, 7(2), 236-247.

[24] Renardy, Y., Popinet, S., Duchemin, L., Renardy, M., Zaleski, S., Josserand, C., ... & Quéré, D. (2003). Pyramidal and toroidal water drops after impact on a solid surface. Journal of Fluid Mechanics, 484, 69-83.

[25] Pasandideh-Fard, M., Qiao, Y. M., Chandra, S., & Mostaghimi, J. (1996). Capillary effects during droplet impact on a solid surface. Physics of Fluids, 8(3), 650-659.

[26] Šikalo, Š., Marengo, M., Tropea, C., & Ganić, E. N. (2002). Analysis of impact of droplets on horizontal surfaces. Experimental Thermal and Fluid Science, 25(7), 503-510.

[27] Cox, R. G. (1986). The dynamics of the spreading of liquids on a solid surface. Part 1. Viscous flow. Journal of Fluid Mechanics, 168, 169-194.

[28] Ramon-Torregrosa, P. J., Rodríguez-Valverde, M. A., Amirfazli, A., & Cabrerizo-Vílchez, M. A. (2008). Factors affecting the measurement of roughness factor of surfaces and its implications for wetting studies. Colloids and Surfaces a: Physicochemical and Engineering Aspects, 323(1-3), 83-93.

[29] Mellero, P., Biegas, S., Carvalho, H., & Ferreira, F. N. (2017). Study of thread tension settings for shirt manufacture using an instrumented lockstich sewing machine.

[30] Brunet, P., Lapierre, F., Zoueshtiagh, F., Thomy, V., & Merlen, A. (2009). To grate a liquid into tiny droplets by its impact on a hydrophobic microgrid. Applied Physics Letters, 95(25), 254102.

[31] Chen, H., Marengo, M., & Amirfazli, A. (2019). Drop impact onto semi-infinite solid surfaces with different wettabilities. Physical Review Fluids, 4(8), 083601.

[32] Lembach, A. N., Tan, H. B., Roisman, I. V., Gambaryan-Roisman, T., Zhang, Y., Tropea, C., & Yarin, A. L. (2010). Drop impact, spreading, splashing, and penetration into electrospun nanofiber mats. Langmuir, 26(12), 9516-9523.

[33] Mangili, S., Antonini, C., Marengo, M., & Amirfazli, A. (2012). Understanding the drop impact phenomenon on soft PDMS substrates. Soft Matter, 8(39), 10045-10054.

[34] Masad, J. A. (1996). Effect of surface waviness on transition in three-dimensional boundary-layer flow.

[35] Joung, Y. S., & Buie, C. R. (2014). Scaling laws for drop impingement on porous films and papers. Physical Review E, 89(1), 013015.

[36] Attané, P., Girard, F., & Morin, V. (2007). An energy balance approach of the dynamics of drop impact on a solid surface. Physics of Fluids, 19(1), 012101.

[37] Muschi, M., Brudieu, B., Teisseire, J., & Sauret, A. (2018). Drop impact dynamics on slippery liquid-infused porous surfaces: influence of oil thickness. Soft Matter, 14(7), 1100-1107.

[38] Lee, C., Kim, H., & Nam, Y. (2014). Drop impact dynamics on oil-infused nanostructured surfaces. Langmuir, 30(28), 8400-8407.

[39] Rothstein, J. P. (2010). Slip on superhydrophobic surfaces. Annual Review of Fluid Mechanics, 42, 89-109.

[40] Kalliadasis, S., Bielarz, C., & Homsy, G. M. (2000). Steady free-surface thin film flows over topography. Physics of Fluids, 12(8), 1889-1898.

[41] https://smithy.com/machining-help/Machining-Reference

[42] Ukiwe, C., & Kwok, D. Y. (2005). On the maximum spreading diameter of impacting droplets on well-prepared solid surfaces. Langmuir, 21(2), 666-673.

[43] Roisman, I. V., Rioboo, R., & Tropea, C. (2002). Normal impact of a liquid drop on a dry surface: model for spreading and receding. Proceedings of the Royal Society of London. Series A: Mathematical, Physical and Engineering Sciences, 458(2022), 1411-1430.

[44] Vallons, K. (2009). The behaviour of carbon fibre–epoxy NCF composites under various mechanical loading conditions. Unpublished doctoral dissertation). Belgium: University Leuven.

[45] Chen, H., Marengo, M., & Amirfazli, A. (2019). Drop impact onto semi-infinite solid surfaces with different wettabilities. Physical Review Fluids, 4(8), 083601.

Appendix A: Fabric deflection measurement

Table A.1: Fabric deflection at drop impact velocity of 2 m/s at different tensions (error for deflections is 0.02 mm)

Tension / Weaving	0.23 N	1.07 N	1.6 N
Satin weave	0.32 mm	0.28 mm (-18 %)	0.26 mm (-25 %)
Warp knit	0.52 mm	0..49 mm (-19 %)	0.47 mm (-27 %)
Weft knit	0.56 mm	0.53 mm (-17 %)	0.51 mm (-23 %)
Plain weave	0.92 mm	0.89 mm (-13 %)	0.87 mm (-20 %)
Mesh weave	1.12 mm	0.95 mm (-12 %)	0.91 mm (-19 %)

Table A.2: Fabric deflection at drop impact velocity of 2.5 m/s at different tensions (error for deflections is 0.02 mm)

Tension / Weaving	0.23 N	1.07 N	1.6 N
Satin weave	0.34 mm	0.31 mm (-18 %)	0.29 mm (-25 %)
Warp knit	0.55 mm	0.52 mm (-19 %)	0.50 mm (-27 %)
Weft knit	0.58 mm	0.55 mm (-17 %)	0.53 mm (-23 %)
Plain weave	0.94 mm	0.91 mm (-13 %)	0.89 mm (-20 %)
Mesh weave	1.18 mm	1.04 mm (-12 %)	0.97 mm (-19 %)

Table A.3: Fabric deflection at drop impact velocity of 3 m/s at different tensions (error for deflections is 0.02 mm)

Tension / Weaving	0.23 N	1.07 N	1.6 N
Satin weave	0.38 mm	0.35 mm (-18 %)	0.33 mm (-25 %)
Warp knit	0.57 mm	0.54 mm (-19 %)	0.52 mm (-27 %)
Weft knit	0.61 mm	0.58 mm (-17 %)	0.56 mm (-23 %)
Plain weave	0.96 mm	0.93 mm (-13 %)	0.91 mm (-20 %)
Mesh weave	1.23 mm	1.04 mm (-12 %)	0.97 mm (-19 %)

Appendix B: Fabrics deflection with time

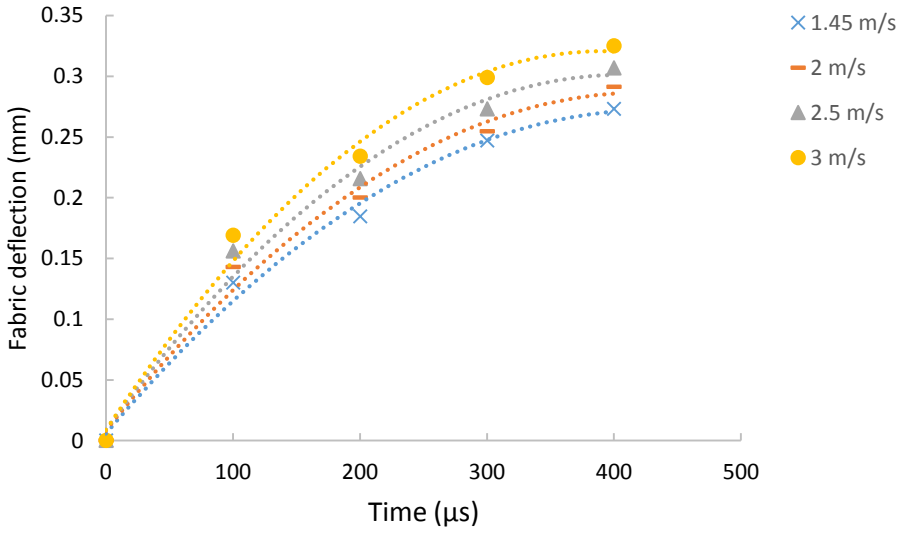

Figure B.1: Deflection of satin weave fabric at impact velocity of 1.45 m/s to 3 m/s at tension of 0.23 N

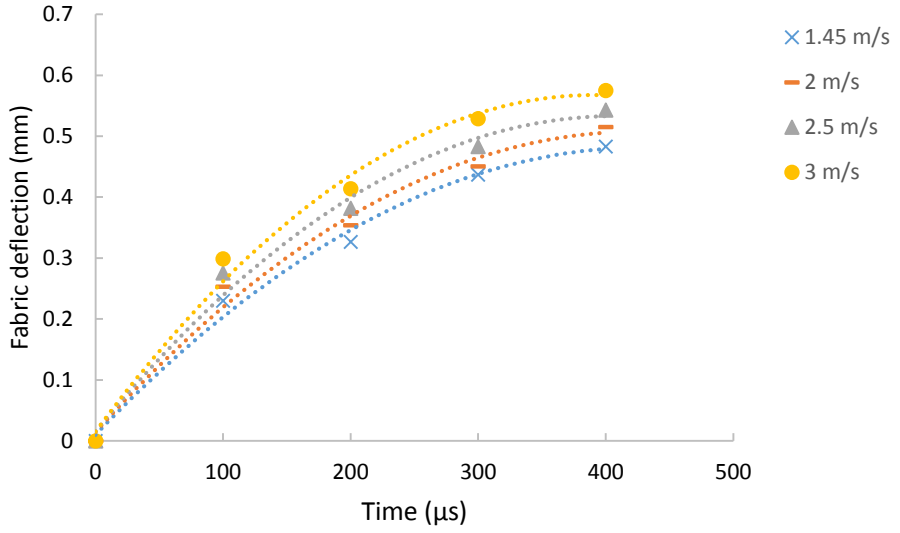

Figure B.2: Deflection of warp knitted fabric at impact velocity of 1.45 m/s to 3 m/s at tension of 0.23 N

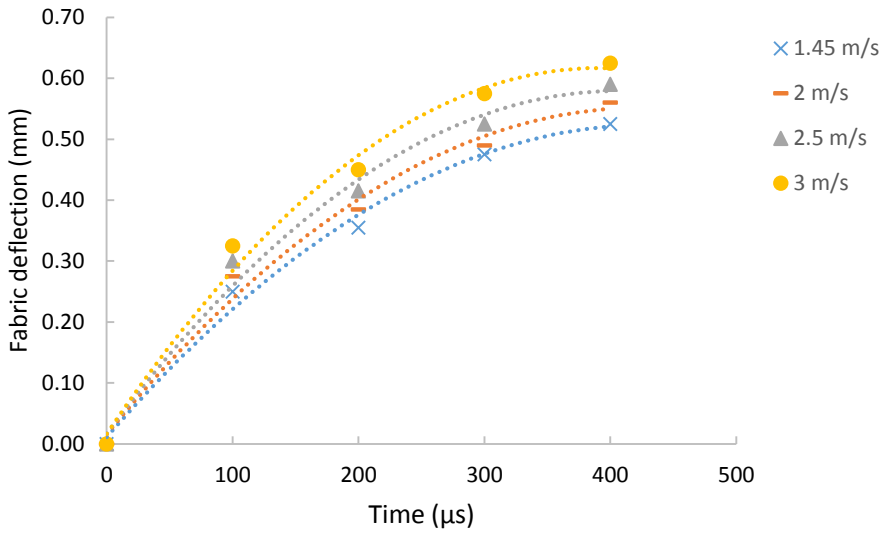

Figure B.3: Deflection of weft knitted fabric at impact velocity of 1.45 m/s to 3 m/s at tension of 0.23 N

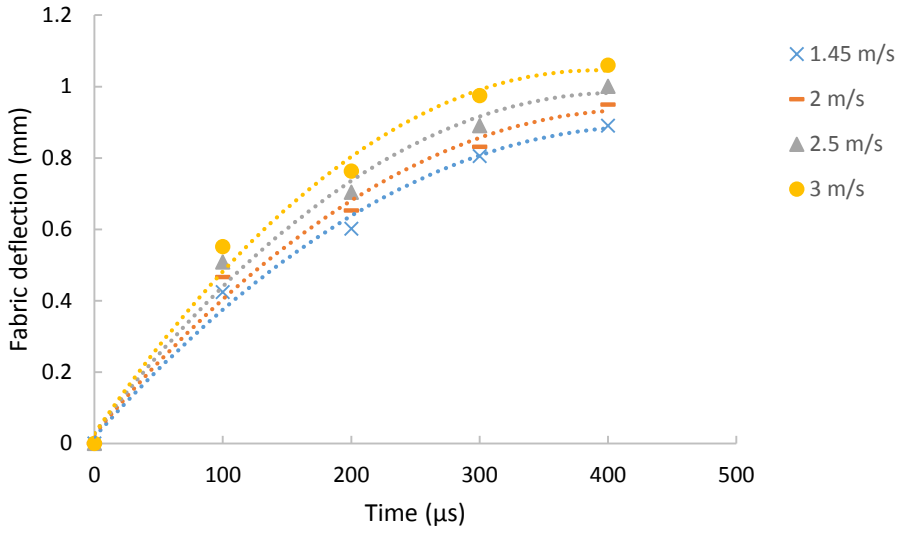

Figure B.4: Deflection of plain weave fabric at impact velocity of 1.45 m/s to 3 m/s at tension of 0.23 N

Appendix C: Fabric deflection with velocity

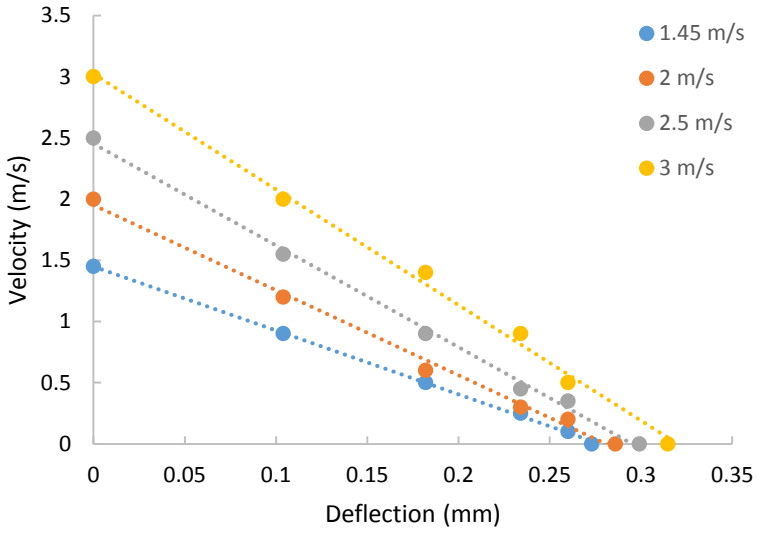

Figure C.1: Deflection of satin weave fabric as a function of velocity at impact velocities of 1.45 m/s to 3m/s, and tension of 0.23 N

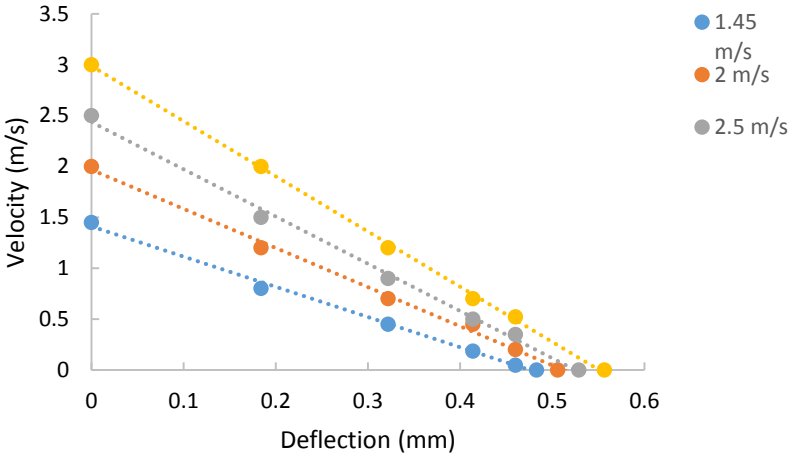

Figure C.2: Deflection of warp knitted fabric as a function of velocity at impact velocities of 1.45 m/s to 3m/s, and tension of 0.23 N

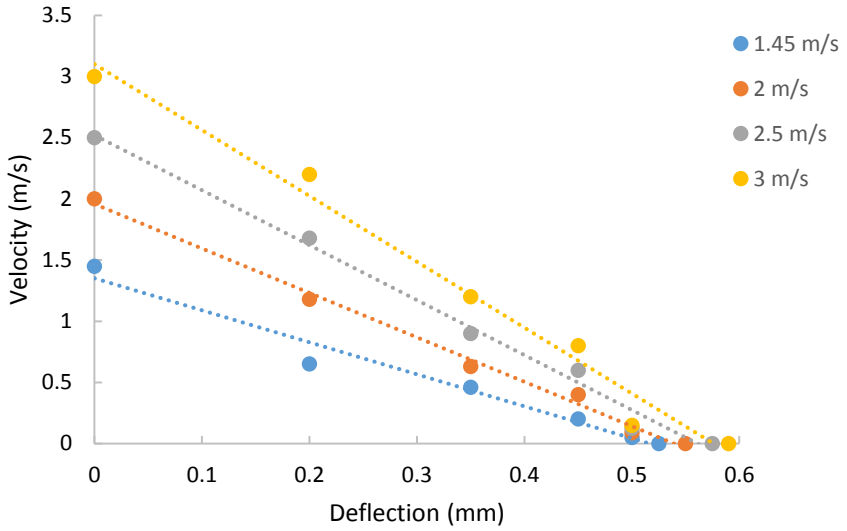

Figure C.3: Deflection of weft knitted fabric as a function of velocity at impact velocities of 1.45 m/s to 3m/s, and tension of 0.23 N

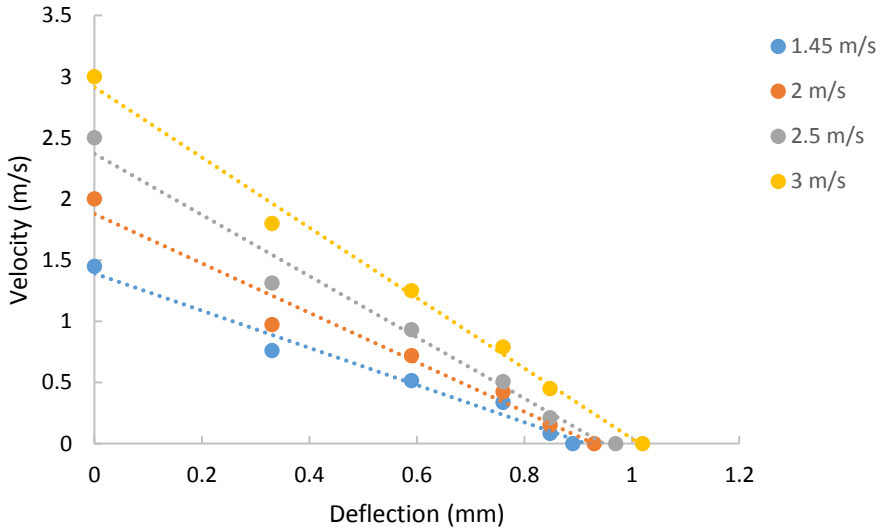

Figure C.4: Deflection of plain weave fabric as a function of velocity at impact velocities of 1.45 m/s to 3m/s, and tension of 0.23 N

Appendix D: Deflection energy

Table D.1: Droplet energy spent for fabric deflection at drop impact velocity of 2 m/s with different tensions

Tension / Weaving	0.23 N	1.07 N	1.6 N
Satin weave	0.009 µJ	0.007 µJ	0.006 µJ
Warp knit	0.016 µJ	0.014 µJ	0.013 µJ
Weft knit	0.018 µJ	0.016 µJ	0.015 µJ
Plain weave	0.025 µJ	0.022 µJ	0.021 µJ
Mesh weave	0.03 µJ	0.027 µJ	0.026 µJ

Table D.2: Droplet energy spent for fabric deflection at drop impact velocity of 2.5 m/s with different tensions

Tension / Weaving	0.23 N	1.07 N	1.6 N
Satin weave	0.011 µJ	0.008 µJ	0.007 µJ
Warp knit	0.021 µJ	0.018 µJ	0.016 µJ
Weft knit	0.024 µJ	0.021 µJ	0.020 µJ
Plain weave	0.031 µJ	0.027 µJ	0.026 µJ
Mesh weave	0.038 µJ	0.035 µJ	0.033 µJ

Table D.3: Droplet energy spent for fabric deflection at drop impact velocity of 3 m/s with different tensions

Tension / Weaving	0.23 N	1.07 N	1.6 N
Satin weave	0.014 µJ	0.012 µJ	0.011 µJ
Warp knit	0.026 µJ	0.023 µJ	0.021 µJ
Weft knit	0.030 µJ	0.027 µJ	0.026 µJ
Plain weave	0.037 µJ	0.035 µJ	0.034 µJ
Mesh weave	0.047 µJ	0.045 µJ	0.044 µJ

Appendix E: Viscous dissipation

Table E.1: Viscous dissipation energy at 2 m/s of drop impact velocity at different tensions

Tension / Weaving	0.23 N	1.07 N	1.6 N
Satin weave	0.38 µJ	0.38 µJ	0.26 µJ
Warp knit	0.39 µJ	0.39 µJ	0.37 µJ
Weft knit	0.39 µJ	0.38 µJ	0.38 µJ
Plain weave	0.37 µJ	0.36 µJ	0.35 µJ
Mesh weave	0.38 µJ	0.38 µJ	0.37 µJ

Table E.2: Viscous dissipation energy at 2.5 m/s of drop impact velocity at different tensions

Tension / Weaving	0.23 N	1.07 N	1.6 N
Satin weave	0.45 µJ	0.43 µJ	0.42 µJ
Warp knit	0.48 µJ	0.46 µJ	0.46 µJ
Weft knit	0.47 µJ	0.45 µJ	0.45 µJ
Plain weave	0.46 µJ	0.44 µJ	0.44 µJ
Mesh weave	0.47 µJ	0.46 µJ	0.46 µJ

Table E.3: Viscous dissipation energy at 3 m/s of drop impact velocity at different tensions

Tension / Weaving	0.23 N	1.07 N	1.6 N
Satin weave	0.52 µJ	0.51 µJ	0.50 µJ
Warp knit	0.54 µJ	0.52 µJ	0.52 µJ
Weft knit	0.53 µJ	0.52 µJ	0.52 µJ
Plain weave	0.55 µJ	0.53 µJ	0.52 µJ
Mesh weave	0.56 µJ	0.55 µJ	0.55 µJ

Appendix F: Surface energy

Table F.1: Surface energies of fabrics at maximum spreading of droplet at drop impact velocity of 2m/s

Tension / Weaving	0.23 N	1.07 N	1.6 N
Satin weave	29.24 µJ	29.60 µJ	29.72 µJ
Warp knit	29.11 µJ	29.35 µJ	29.44 µJ
Weft knit	29.16 µJ	29.29 µJ	29.37 µJ
Plain weave	29.82 µJ	30.05 µJ	30.17 µJ
Mesh weave	29.62 µJ	29.79 µJ	29.82 µJ

Table F.2: Surface energies of fabrics at maximum spreading of droplet at drop impact velocity of 2.5m/s

Tension / Weaving	0.23 N	1.07 N	1.6 N
Satin weave	45.03 µJ	45.19 µJ	45.28 µJ
Warp knit	44.82 µJ	45.01 µJ	45.08 µJ
Weft knit	44.87 µJ	45.06 µJ	45.11 µJ
Plain weave	44.49 µJ	44.7 µJ	44.79 µJ
Mesh weave	44.27 µJ	44.41 µJ	44.5 µJ

Table F.3: Surface energies of fabrics at maximum spreading of droplet at drop impact velocity of 3m/s

Tension / Weaving	0.23 N	1.07 N	1.6 N
Satin weave	64.06 µJ	15.89 µJ	15.89 µJ
Warp knit	15.95 µJ	15.97 µJ	15.97 µJ
Weft knit	15.94 µJ	15.96 µJ	15.96 µJ
Plain weave	15.85 µJ	15.81 µJ	15.81 µJ
Mesh weave	15.74 µJ	15.70 µJ	15.69 µJ

Appendix G: Time for reaching maximum diameter

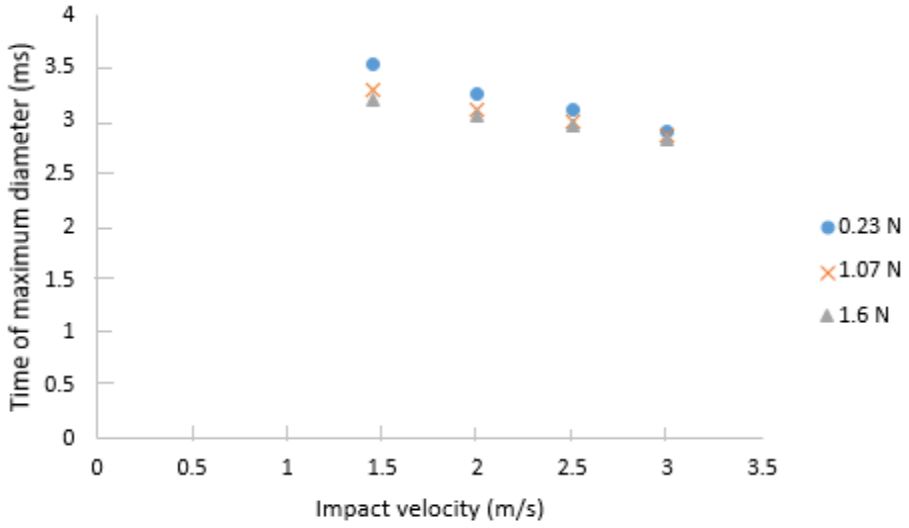

Figure G.1: Time for reaching maximum diameter for Warp knit

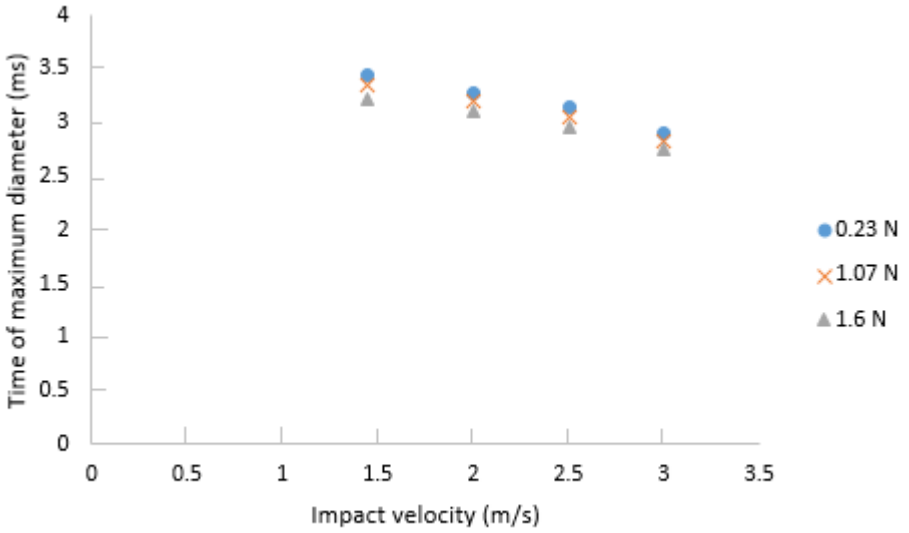

Figure G.2: Time for reaching maximum diameter for Weft knit

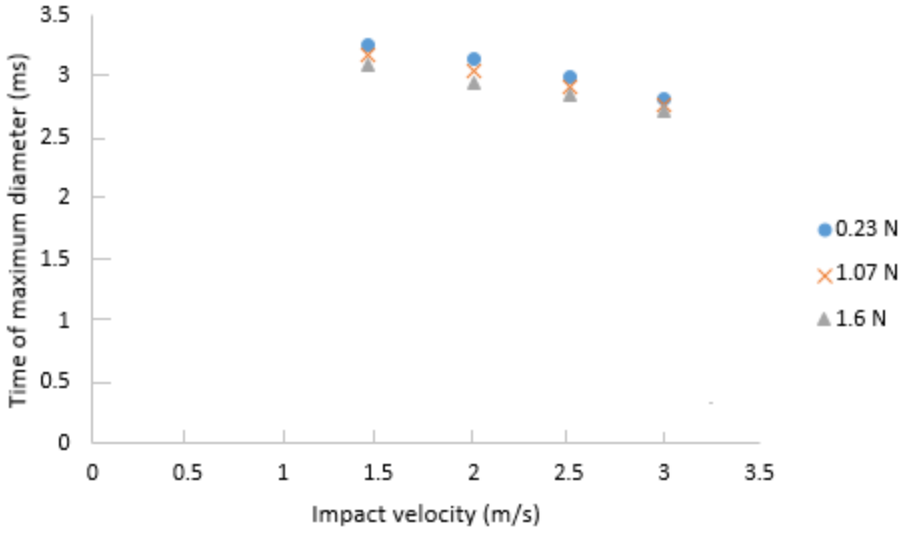

Figure G.3: Time for reaching maximum diameter for Plain weave

Appendix H: Sample calculations

Warp knit at impact velocity of 1.45 m/s and 0.23 N of tension has been considered as a sample for calculation. All experiments have been done for three times. At each time, all parameters like impact velocity, droplet diameter, maximum spreading, etc. has been measured and their average has been considered as the amount for each parameter. It is obvious that the discrepancy between measured parameters is considered as the error.

$E_{s1}=4.\ \Pi.r^2.\ \Upsilon_{lv}$ (H.1)

r=1.5mm (± 0.03 mm) (H.2)

$\Upsilon_{lv}=72.9\times10^{-3}$N/m (H.3)

$E_{s1}=4.\ \Pi.(0.0015)^2\times72.9\times10^{-3}$= 2.05 μJ (± 0.1 μJ) (H.4)

$E_{k1}=0.5\times m\times V^2$ (H.5)

V=1.45 m/s (± 0.02 m/s) (H.6)

ρ =1000 kg/m^3 ; r= 1.5 mm (± 0.03 mm) (H.7)

Mass of droplet (m)= $\rho.\ 4/3\pi.r^3$= 1.41e-5 (± 0.08 e-5) (H.8)

Thus E_{k1}=14.8 μJ (± 0.5 μJ) (H.9)

r_v=0.01 (H.10)

Thus $E_p=r_v.E_{k1}$= 0.01 ×14.8=0.14 μJ (± 0.05 μJ) (H.11)

$E_e=\int F.dt.dx$= m. Δv. Δx (H.12)

ρ =1000 kg/m^3 ; r= 1.5 mm (± 0.03 mm) (H.13)

ΔV =1.45 m/s (± 0.02 m/s) (H.14)

Δx = 0.49 mm (± 0.02mm) (H.15)

Thus E_e= 1.41e-5 × 1.45 m/s ×0.49×10^{-3}=0.011μJ (± 0.0008 μJ) (H.16)

$E_v=\int \tau . V . dA$= work. Time=P. Δt=[3 (Ψ/We).$R_{max}{}^2$.($\Delta r/\Delta t)^2$.A_s/A_p]. Δt (H.17)

$\Psi= \pi/(oh)^{0.5}$ (H.18)

μ = 8.9×10^{-4} Pa.s (H.19)

Oh=$\sqrt{We}/Re$=$\sqrt{90}$/4591=0.002 (± 0.00017) (H.20)

Ψ=70.24 (H.21)

R_{max}=4 mm (± 0.2 mm) (H.22)

Δr =4mm-1.5mm=2.5mm (H.23)

Δt =3540 μs (± 130 μs) (H.24)

As/Ap=3.2 (H.25)

E_v=0.22 μJ (± 0.016 μJ) (H.26)

Model used by Joung and Buie:

$E_v=\int \tau . V . dA$= (π/2).(π/Oh)$^{0.5}$. μ/D_0.$R_{max}{}^2$.$(dR/dt)^2$.As/Ap. Δt (H.27)

By putting all values in equation above:

E_v=0.29 μJ (± 0.019 μJ) (H.28)

The reason for using the term A_s/A_p is discussed completely in waviness section.

$$E_{S2}=\Upsilon_{lv}.\pi.R_{max}^{2}+\Upsilon_{sl}.\pi.R_{max}^{2}.\frac{As}{Ap} \quad \text{(H.29)}$$

$\Upsilon_{lv}=72.9\times10^{-3}$ N/m at 20 ^{0}C (H.30)

$\Upsilon_{sv}=38\times10^{-3}$ & contact angle: 92^0 (H.31)

$\Upsilon_{sl}=73.5\times10^{-3}$ N/m (H.32)

R_{max} (maximum spreading of droplet) = 4 mm (± 0.2 mm) (H.33)

As/Ap=3.2 (H.34)

$E_{S2=}$16.2 μJ (± 0.7 μJ) (H.35)

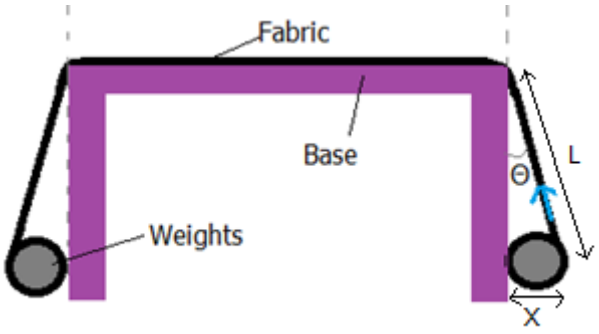

Figure H.1: Schematic view of fabric and the applied tension

L = 8.26 cm (H.36)

X= 1.1 cm (H.37)

$\theta = Sin^{-1}(X/L)= Sin^{-1}(0.13) = 7^0$ (H.38)

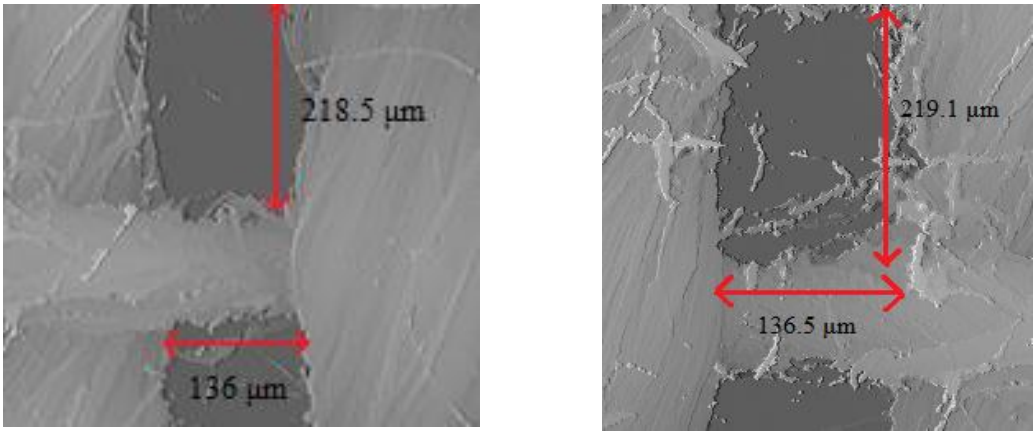

(a) (b)

Figure H.2: Plain weave Voids size at fabric tension of a. 023 N and b. 1.06 N.

As it is shown in Figure H.2, by increasing tension no considerable changes can be seen in voids size.

In order to measure the maximum diameter in cases that splashing happened, it is tried to find the whole area which is covered by the droplet liquid (red areas in Figure H.3); then, the diameter of a circle with the same area as droplet covered area has been considered as droplet maximum diameter (black circle in Figure H.3).

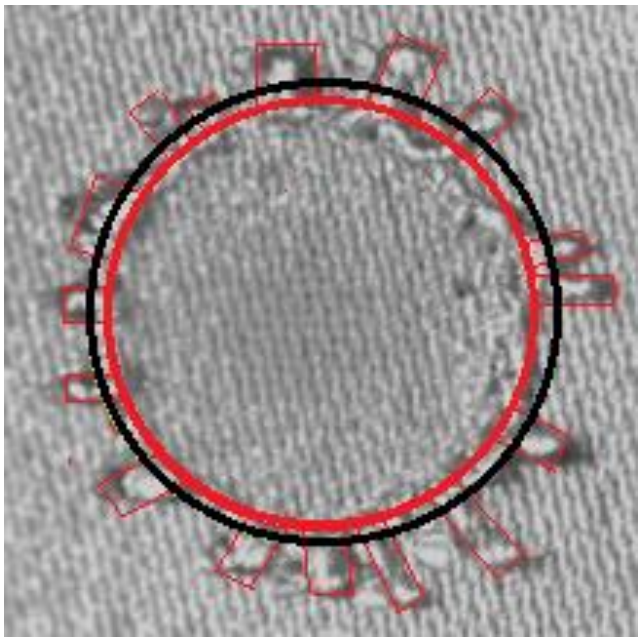

Figure H.3: Image processing for maximum droplet diameter calculation

Thus

$$\text{Droplet area} = A_{\text{red circle}} + \Sigma\,(A_{\text{rectangles}}) = A_{\text{black circle}} = \pi.\,(r_{\text{black circle}})^2 \qquad \text{(H.39)}$$

In order to calculate the errors, each experiment has been done three times. In each of these experiments, maximum spreading of droplet is measured based on mentioned method. The average of measured diameters is considered as the maximum spreading diameter; then, the discrepancy between the mean diameter and measured diameters is considered as the error of measurements.